An examination of interacting residues in the GABA-gated ion channel UNC-49 within the parasitic nematode *Haemonchus contortus*

By

Everett Cochrane

A Thesis Submitted in Partial Fulfillment of the Requirements for the Degree of

Masters of Science

In

The Faculty of Science

Applied Bioscience

University of Ontario Institute of Technology

October 2017

Certificate of Approval

Abstract

Haemonchus contortus is a blood-feeding parasitic nematode that infects ruminant animals around the world, including those with significant economic importance such as cattle, sheep, and goats. UNC-49 is a GABA-gated chloride channel found to be exclusive to nematodes which could be a viable future target for anthelminthic drugs. An analysis of the model of the Hco-UNC-49 receptor has identified potentially interacting residues that may be important to its structure and function. One such potential interaction between K181 and E183, which appears to be unique to nematode GABA receptors, was selected for study based on charge and proximity to each other and the ligand binding site. A variety of mutations at these positions were introduced and analyzed by two-electrode voltage clamp electrophysiology. It was found that both residues are important for receptor function, but modifications to the E183 residue yielded a greater negative impact. It was also found that K181 and E183 are energetically coupled suggesting that they interact possibly through a salt-bridge. Disulfide trapping indicated that the two residues are in close enough proximity to directly interact. This analysis of key residues in a unique receptor could potentially be utilized for the future development of new anthelmintics to combat the increasing prevalence of infection by *H. contortus*.

Keywords: *Haemonchus contortus*, UNC-49, cys-loop receptor, GABA, electrophysiology, salt bridge, mutant cycling, disulfide trapping

Acknowledgements

I would first like to thank Dr. Sean Forrester for giving me this opportunity and welcoming me into his lab. It has been a wonderful experience working and studying at UOIT and I couldn't have asked for a better supervisor.

Thank you, Micah Callanan, for passing on your knowledge of pharmacology and always having helpful advice when I couldn't figure out what to do next.

Thank you, Josh Foster, for showing me the ropes in the lab and teaching me how to do many of the things I've done in my time here. Thanks for sharing in my unique sense of humour and being a great conversation partner for all the long days spent in the lab.

Thank you, Sarah Abdelmassih, for all your hard work and for bringing some of the best organizational skills into the lab. All the ways we've improved electrophysiology will surely be useful for years to come.

Thanks to all the undergraduate thesis and summer research students I've worked with throughout the last two years, especially Siddiq, Kristen, and Aloka. Your contributions did not go unnoticed.

Thanks to the fourth-floor labs for making every day awesome and providing great conversations in 'Matt's' corner. We have a great community here and I'll never forget it.

Lastly, thank you to my friends and family for their never-ending support, even if they only tell people that I'm "trying to save the world from vampire goat-worms." Thanks for always being interested (or pretending to be!) in what I was saying even if you didn't fully understand it.

Table of Contents

List of Tables

List of Figures

Appendices

List of Abbreviations

Cel-UNC-49	*Caenorhabditis elegans* uncoordinated gene 49 GABA receptor
cRNA	Copy RNA
Cys-loop	Cysteine loop
[D]	Concentration of the agonist
DAVA	5-aminovaleric acid
EC_{50}	50% of maximal response
ECD	Extracellular domain
GABA	γ-Aminobutyric acid
$GABA_A$	Vertebrate heteromeric GABA-gated chloride channel
$GABA_C$	Vertebrate homomeric GABA-gated chloride channel
h	Hill slope
Hco-UNC-49B	*Haemonchus contortus* uncoordinated gene 49 homomeric receptor
Hco-UNC-49BC	*Haemonchus contortus* uncoordinated gene 49 heteromeric receptor
ICD	Intracellular domain
IMA	Imidazole-4-acetic acid
LGIC	Ligand gated ion channel
M1-4	Transmembrane domains 1 through 4
MS-222	3-aminobenzoic acid ethyl ester methane sulphonate salt
n	Number of replicates
NAM	Negative allosteric modulator
PS	Pregnenolone Sulfate
RDL	*Drosophila melanogaster* GABA-gated chloride channel
R-GABOB	(R)-(-)-4-Amino-3-hydroxybutyric acid
S-GABOB	(S)-(+)-4-Amino-3-hydroxybutyric acid
TEVC	Two-electrode voltage clamp
TMD	Transmembrane domain

Introduction

Section 1: Introduction

1.1 Introduction to *Haemonchus contortus*, a Parasitic Nematode

Haemonchus contortus is a free-living parasitic nematode of the order Strongylida, which infects ruminants such as sheep and goats. *H. contortus* comes from the same phylum, Nematoda, as the well-studied free-living nematode, *Caenorhabditis elegans* (Blaxter et al., 1998). *H. contortus* parasites feed on the blood of the host by attaching to the inside lining (mucosa) of the abomasum, the fourth stomach compartment found in ruminants. Once infected via ingestion, affected animals begin to experience symptoms such as anemia and other digestive complications potentially leading to death (Nikolaou & Gasser, 2006). These complications can lead to a variety of economically damaging side effects including but not limited to a reduction in milk and wool production (Qamar et al., 2011).

Since first being studied in 1915 by Dr. Frank Veglia, *H. contortus* has been found in many countries around the world raising a global concern. Infection with *H. contortus* was initially thought to be primarily located in tropical or sub-tropical areas, but recent years have shown an increased occurrence of infections in temperate zones (Akkari et al., 2013). This may be in part due to the parasite's resilience to temperature changes and its ability to halt development within the host during the fourth larval stage until external conditions become favourable (Manninen et al., 2008).

1.2 Life Cycle of *Haemonchus contortus*

The life cycle of *H. contortus* progresses through five primary stages, denoted as L1 through L5. Adult females in the L5 stage begin a new life cycle when they lay eggs

within the abomasum of infected ruminant animals (Veglia, 1915). The eggs move through the animal's digestive system naturally and exit the host in the feces. The embryos are unable to develop inside the host because they require oxygen that is unavailable within the abomasum (Nikolau & Gasser, 2006). Once outside the host, the eggs hatch within the feces and the nematode enters the free-living larval stage L1. The larvae begin moving around in search of food, such as bacteria from within the feces. Once fed, the L1 larvae dig deeper into the feces to find moisture and protection from direct sunlight, after which they enter a lethargic phase where growth and cellular division eventually lead to the second stage, L2 (Veglia, 1915). The L2 larvae proceed with a second round of feeding before entering another lethargic phase allowing for the development of the mouth, oesophagus, and intestines (Veglia, 1915). Now in the third larval stage, L3, the larvae detach themselves from their old skin and are able to move around freely. The larvae move to nearby vegetation, resting on grass or plants that are eventually consumed by ruminants. The ingested L3 larvae develop into the L4 stage once inside the host (within 48 hours of ingestion) (Veglia, 1915). Here they develop the mouth parts, such as a tooth-like lancet, that are necessary to pierce the stomach lining and feed on the host's blood. Feeding on blood allows *H. contortus* to grow into the final mature adult form, L5 (Veglia, 1915). From here the cycle begins again as mature females are able to lay 4500 eggs every day (Nikolau & Gasser, 2006).

1.3 Control of *Haemonchus contortus*

H. contortus infections are generally treated through the use of anthelmintics, which are a group of antiparasitic drugs that target helminths (parasitic worms). One major concern with the continued use of such drugs is the development of anthelmintic

resistance. Though the appearance of resistance can be reduced by following the appropriate guidelines for each drug and proper cycling of different anthelmintic classes, many areas in the world do not follow these practices, leading to unacceptably high resistance problems (Newton, 1995). Many compounds have been used in an effort to combat the effects of *H. contortus*. Some of these are described below.

1.3.1 Benzimidazoles

Benzimidazoles were one the most widely used classes of antiparasitic drugs for an extensive period of time before better alternatives, such as macrocyclic lactones were found (Blackhall et al., 2008). They act by binding β-tubulin with high affinity and specificity, which causes a depolymerization of microtubules that are important for muscle function allowing for motility (Blackhall et al., 2008). Resistance to benzimidazoles in *H. contortus* has been found to be linked with genes that encode β-tubulin. This correlation can also be seen in other organisms such as fungi or the closely related free-living nematode, *Caenorhabditis elegans* (Blackhall et al., 2008). The structure of the benzimidazole, albendazole, can be seen in Figure 1.

1.3.2 Cholinergic Agonists (Imidizothiazoles)

Cholinergic agonists act on acetylcholine-gated ion channels found within the body muscles of nematodes (Boulin et al., 2011). These drugs function by activating acetylcholine receptors, keeping the ion channel open for an extended period of time and inducing a state of paralysis in the parasite via continuous muscle contraction (Martin et al., 1997). Paralyzed nematodes become unable to stay attached to the host and will eventually pass through the animal's digestive system naturally (Charvet et al., 2012).

Levamisole is one such example of an imidizothiazole used to treat ascariasis and hookworm (Figure 1).

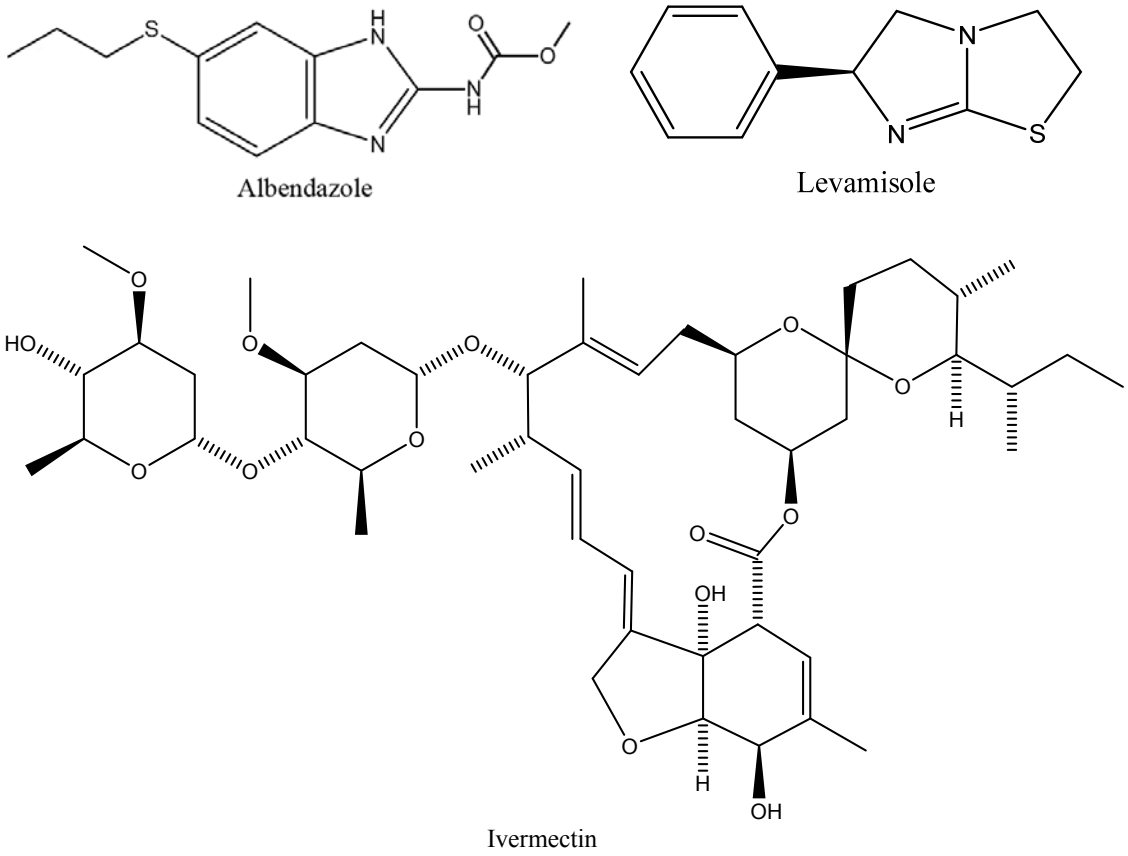

Figure 1: Some compounds utilized as anthelmintics to combat infection by *H. contortus*.

1.3.3 Macrocyclic Lactones (Avermectins)

Macrocyclic lactones from the avermectin family are compounds that act on the glutamate-gated chloride (GluCl) channels that are exclusive to invertebrates such as nematodes (Martin et al., 1997). These compounds bind the GluCl channels essentially irreversibly to cause an increase in chloride ions across the membrane. This causes a hyperpolarization of neuromuscular cells in the target organism that results in paralysis

(Blackhall et al., 2008). One example of a drug in this category is ivermectin (Figure 1) which was discovered in the 1970s and is a common ingredient in antiparasitic medications for farm animals as well as pets such as cats and dogs (Elgart & Meinking, 2003).

1.4 Ligand-gated Ion Channels

Ligand-gated ion channels (LGICs) function by recognizing specific neurotransmitters and mediating a rapid response at the synapse (Unwin, 1993). These channels are comprised of several transmembrane proteins, which allow neurotransmitters to bind in order to initiate a conformational change to the open state. Once in the open state, the LGIC forms an aqueous channel between one side of the membrane and the other allowing ions to flow across the electrochemical gradient. The changing electric potential between the two sides of the membrane causes a response within the target cell (Unwin, 1993).

LGICs can function at excitatory synapses by allowing the passage of cations (such as with acetylcholine or serotonin receptors), or at inhibitory synapses allowing the passage of anions (as seen with GABA receptors) (Unwin, 1993). These channels can be found in the nervous systems of vertebrates as well as invertebrates such as *H. contortus* and they play an important role in the control of muscles required for locomotion and feeding (Komuniecki et al., 2012).

1.5 Cysteine-loop LGICs

Within the LGICs there is a superfamily of receptors known as cys-loop LGICs. These include several receptors such as those for acetylcholine and γ-Aminobutyric acid

(GABA). They can be found in large concentrations at the nerve-muscle synapse (Unwin et al., 2002). These LGICs are defined by a specific loop located in the N-terminal extracellular domain (ECD) formed by a disulfide bond between two cysteine residues (Thompson et al., 2010). These cysteine residues are spaced 13 amino acids apart, a trait found to be conserved among all cys-loop receptors (Cascio, 2004).

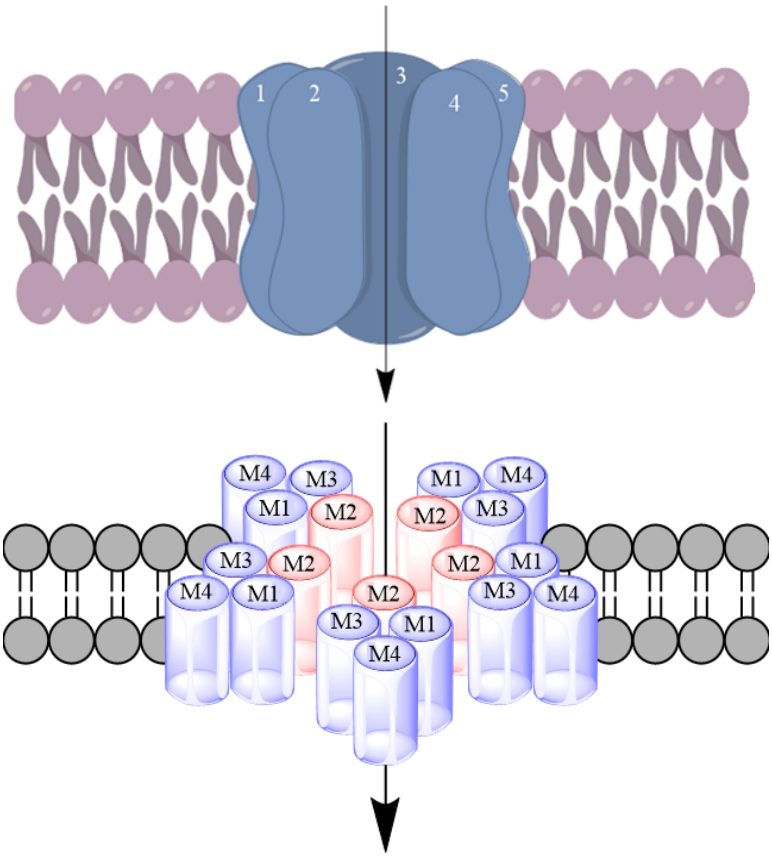

Figure 2: **Top**: General structure of LGICs - five subunits arranged pseudosymetrically around the central channel. Subunits highlighted 1-5 for clarity. **Bottom**: Position of M1-M4 domains for each subunit surrounding the channel, with M2 domains facing the central channel. The arrow indicates the direction of ion flow once in the open state.

Cys-loop LGICs have a shared structure made up of five subunits arranged pseudo-symmetrically around a central channel, which can conduct the flow of ions once in the open state (Cascio, 2004; Thompson et al., 2010) (Figure 2). Each of the five

subunits of the receptor has four transmembrane domains (TMD), a large N-terminal extracellular domain, and an extended cytoplasmic loop in the intracellular domain (ICD) (Unwin, 2002) (Figure 3). The ligand binding site can be found in the large N-terminal extracellular domain, between 3 loops of the primary subunit and 3 β-sheets of an adjacent complimentary subunit (Thompson et al., 2010). The loops are referred to as A, B, and C in the primary subunit, and D, E, and F in the complimentary subunit. These loops contain aromatic residues (phenylalanine, tryptophan, and tyrosine) which allow for cation-π interactions with the ligand (Thompson et al., 2010). This type of interaction occurs when the aromatic rings create an electrostatic potential that is negative in the middle and positive on the outer ring (Dougherty, 2007). The result is an attraction of cations towards the negatively charged center, effectively holding the ligand in place.

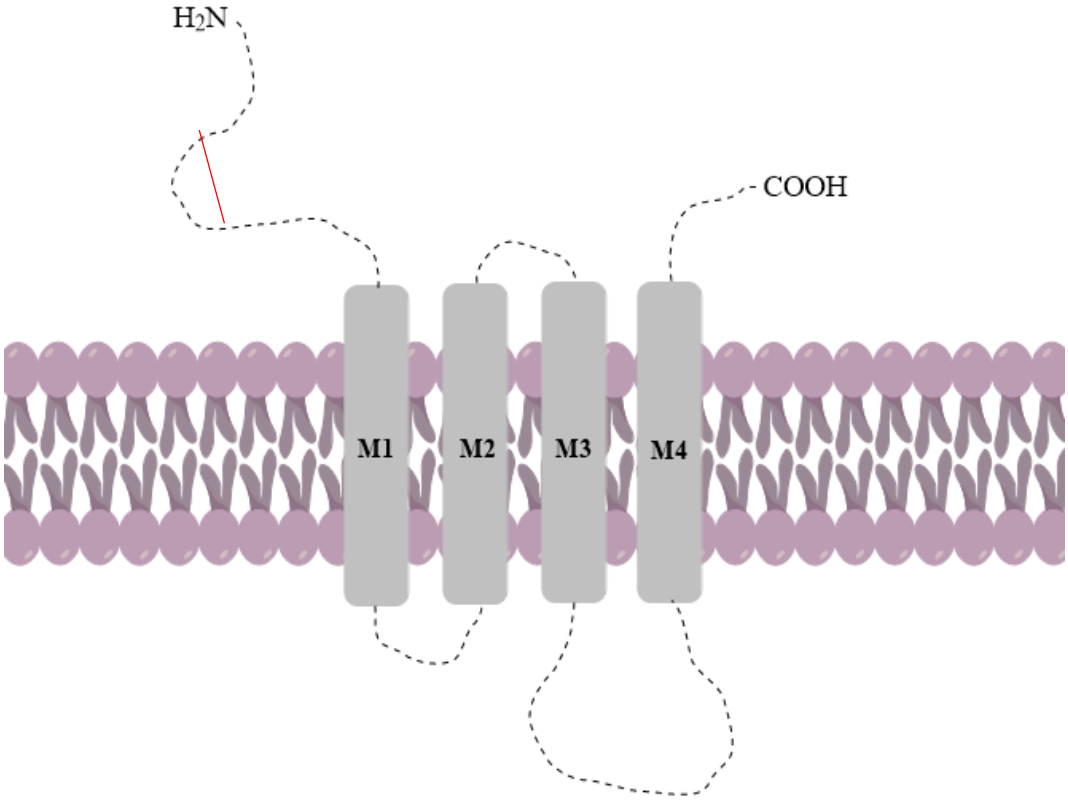

Figure 3: A visualization of the 4 transmembrane domains found within a single subunit of a cys-loop ligand-gated ion channel. The red line indicates the disulfide bond between the two cysteine residues that are characteristic of this channel type.

The transmembrane domain of each subunit is comprised of four α-helices spanning the membrane, numbered M1 through M4. The M1, M3, and M4 segments surround and protect the inner M2 region from its surroundings (Figure 2). The M2 α-helix of each subunit come together to form the central pore, which is important since this segment is responsible for selecting which ions are able to pass through the channel (Thompson et al., 2010). It is thought to be caused by a small kink formed by a few residues in the M2 domain which allow it to restrict the flow of chloride ions (Unwin, 2005). The loop between the M2 and M3 domain is important for connecting the ECD with the TMD and assists with opening the channel once a ligand is bound (Thompson et al., 2010). This occurs via a destabilization of a hydrophobic region within the channel, which moves away from the center and allows the passage of ions to occur (Thompson et al., 2010).

1.6 γ-Aminobutyric acid

γ-Aminobutyric acid (GABA) (Figure 4) is a neurotransmitter which plays a critical role in the nervous systems of many organisms. It is the primary inhibitory neurotransmitter in mammals responsible for inhibiting nerve transmission in the brain to reduce neuronal activity (Bamber et al., 2003). GABA is synthesized in the brain via the conversion of the primary excitatory neurotransmitter glutamate, and is eventually converted back into glutamate via a metabolic pathway called the GABA shunt (Olsen & DeLorey, 1999). Inhibitory and excitatory functions are reliant on a balance between their respective neurotransmitters. An improper balance in excitatory and inhibitory neurotransmission in vertebrates can lead to severe consequences, such as seizures or loss of consciousness (Schuske et al., 2004). Though GABA is known to be inhibitory in

mammals and other vertebrates, it has been found to have some excitatory functions in invertebrates, such as nematodes (Accardi et al., 2012). Several GABA receptor agonists have been used to analyze the pharmacological profile of various GABA receptors, including R-(-)-4-amino-3-hydroxybutyric acid (R-GABOB), S-(+)-4-amino-3-hydroxybutyric acid (S-GABOB), imidazole-4-acetic acid (IMA), and 5-aminovaleric acid (DAVA) (Kaji et al., 2015) (Figure 4).

1.7 GABA in Invertebrates

Nematodes, such as *C. elegans* and *H. contortus*, rely on GABA for locomotion. GABA has been found to act on neuromuscular junctions in *C. elegans* rather than the central nervous system in vertebrates (Schuske et al., 2004). Nematodes are able to bend and move around by contracting muscles on one side of the body via excitatory acetylcholine stimulation while simultaneously relaxing the muscles on the other side via inhibitory GABA stimulation. Excitatory GABA stimulation in *C. elegans* allows the release of waste through a series of muscle contractions along the body occurring every 50 seconds, forcing intestinal waste towards the tail end of the worm to be excreted (Schuske et al., 2004). A failure of inhibitory GABA receptors could result in the nematode being paralyzed and unable to relax contracted muscles, whereas a failure of excitatory GABA receptors could result in the nematode being unable to release waste. Both of these possibilities provide a good incentive for further analysis of the invertebrate GABA receptor, particularly when considering harmful parasitic invertebrates.

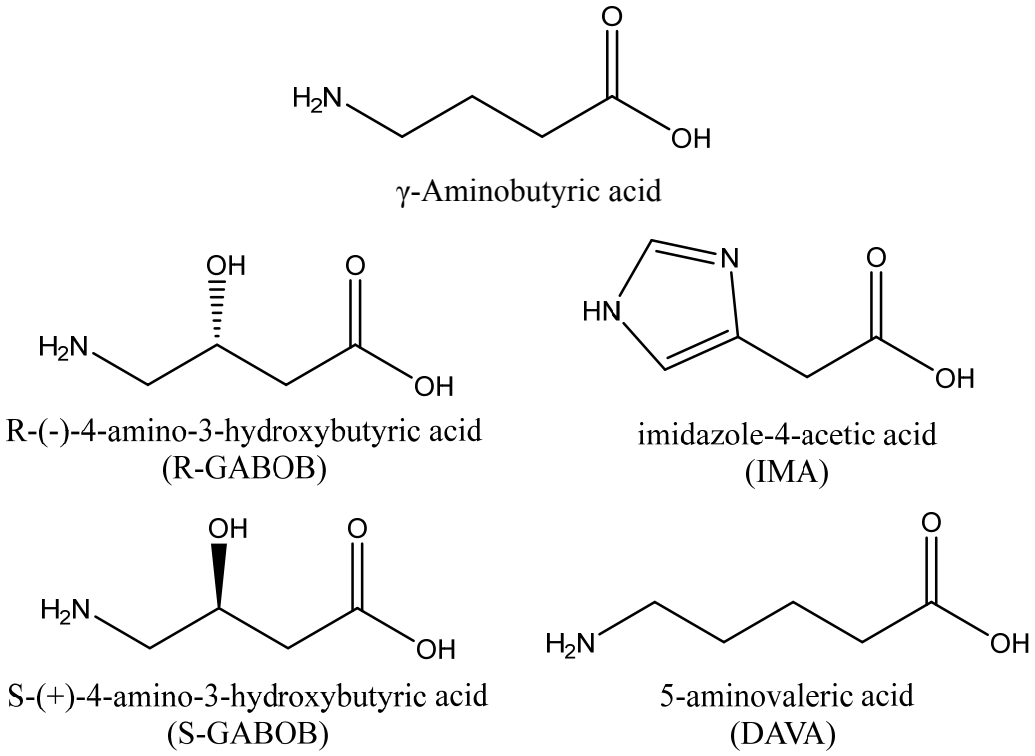

Figure 4: Chemical structures of GABA and GABA receptor agonists.

1.8 GABA Receptors in Vertebrates

This family of receptors responds to the major inhibitory neurotransmitter of the vertebrate central nervous system, GABA. GABA receptors can be split into two primary subclasses, LGICs (ionotropic) which include $GABA_A$ and $GABA_C$, and G-protein coupled receptors (GPCRs, metabotropic) which include $GABA_B$ (Jones et al., 1998). Each of these receptor types have unique properties. $GABA_A$ have been shown to exhibit a sensitivity to the antagonist bicuculline. $GABA_B$ receptors can be activated by a GABA analog called baclofen (Zhang et al., 2001). $GABA_C$ receptors, which were found to exist in both vertebrates and invertebrates, are insensitive to both bicuculline and baclofen, and can activated by enantiomers of the GABA analog, 4-aminocrotonic acid (Zhang et al.,

2001). $GABA_A$ receptors are critical for inhibitory signaling in the central nervous system.

1.9 $GABA_A$ Receptors

$GABA_A$ receptors in vertebrates are pentameric in nature, with a large number of subunits that can form receptors of varying functions. Different combinations of subunits can result in varying pharmacological properties, among other changes (Sieghart, 1995). Human $GABA_A$ receptors have eight classes of subunits (α1-6, β1-3, γ1-3, δ, ε, θ, π, and ρ1-3), which are encoded by 19 different genes (Miller & Aricescu, 2014). Though there are a large number of potential subunit combinations, the actual amount is limited by strict assembly rules that seek energetically favoured subtypes. The most common assembly for heteromeric $GABA_A$ receptors are two α subunits, two β subunits, and one final subunit that is most commonly a γ subunit (Miller & Aricescu, 2014). Though these receptors can form functional homomeric channels with five β3 subunits, they are not commonly found throughout the brain (Miller & Aricescu, 2014). The homomeric channel is however useful for modelling purposes (Figure 5), which may be able to provide structural information applicable to other models. $GABA_A$ receptors have been used as drug targets in humans for treatment of various conditions such as epilepsy, insomnia, and anxiety (Miller & Aricescu, 2014). Like other cys-loop LGICs, each subunit is comprised of 4 TMDs (M1-M4), and the ligand binding site is formed between loops A, B, and C of the principle subunit, and loops D, E, and F of the secondary subunit (Accardi & Forrester, 2011).

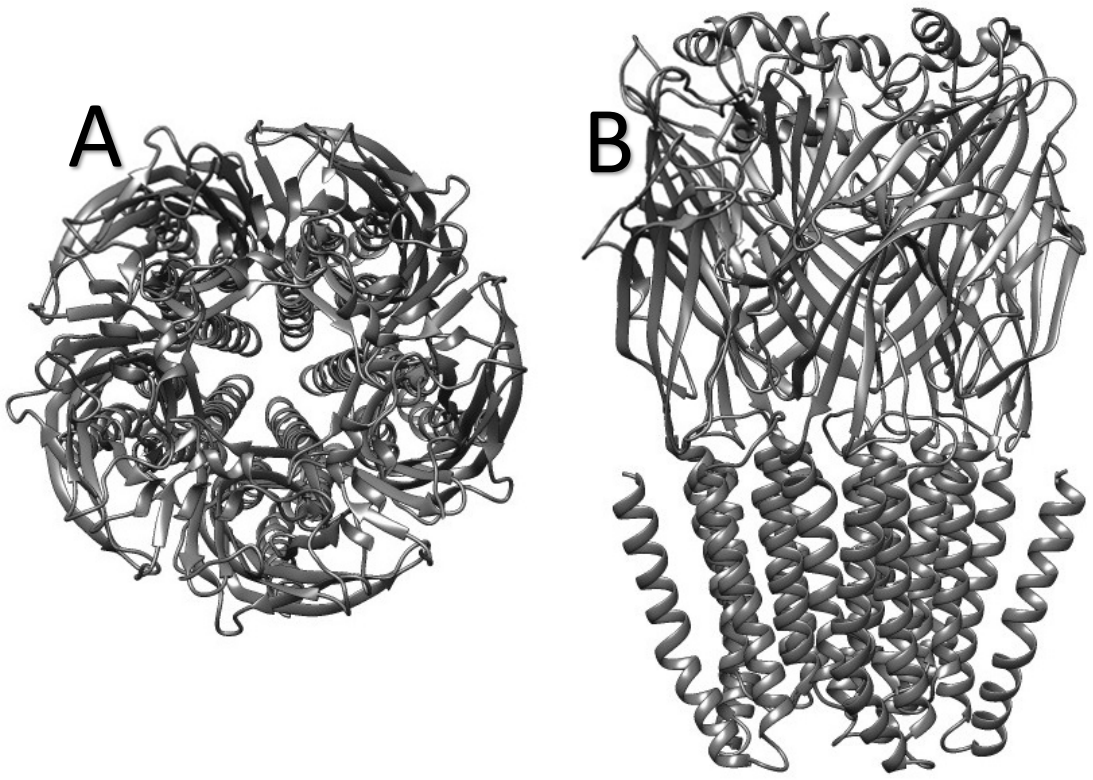

Figure 5: Crystal structure of the human homomeric $GABA_A$ β3 receptor. **A**, Top view. **B**, Side view. PDB 4COF (Miller & Aricescu, 2014).

1.10 UNC-49 Receptor in Nematodes

In *C. elegans*, *H. contortus*, and other free-living nematodes, the primary inhibitory GABA receptor is UNC-49. This GABA receptor is encoded by the *unc-49* gene. The gene encodes three distinct UNC-49 subunits in *C. elegans*, which have differences primarily in their C-terminus, and are identified as Cel-UNC-49A, Cel-UNC-49B, and Cel-UNC-49C (Bamber et al., 1999). The Cel-UNC-49A subunit is not expressed in significant levels, whereas the B and C subunits appear to play a more important role. Cel-UNC-49B has the ability to form homomeric channels with other B subunits, however in *C. elegans*, the heteromeric Cel-UNC-49B/C channel is the native

form (Bamber et al., 1999). The Cel-UNC-49C subunit can only form heteromeric channels with the B subunit, and does not form a homomeric channel.

1.11 UNC-49 Receptor in *H. contortus*

Although the UNC-49 receptor in *H. contortus* has not been studied as extensively as the closely related *C. elegans*, it has proven to be a good comparative model. *H. contortus* has been found to share two of the UNC-49 subunits found in *C. elegans*, which are Hco-UNC-49B and Hco-UNC-49C. These two subunits are very highly conserved between the two species, but some key differences have been shown in their functionality. The *C. elegans* heteromeric UNC-49B/C channel shows decreased GABA sensitivity compared to the homomeric unc-49B channel, whereas the *H. contortus* heteromeric channel shows increased GABA sensitivity (Siddiqui et al., 2010). The reverse holds true for the homomeric channel. However, the exact cause for this is not known. The UNC-49C subunit appears to carry resistance to the channel blocker picrotoxin, which is attributed to a key methionine residue in the M2 domain of UNC-49C (Siddiqui et al., 2010). Like mammalian $GABA_A$ receptors, the GABA binding site is found between two adjacent subunits and is stabilized by loops in both the principle and complementary subunits (Accardi & Forrester, 2011). A model of this can be seen in Figure 6.

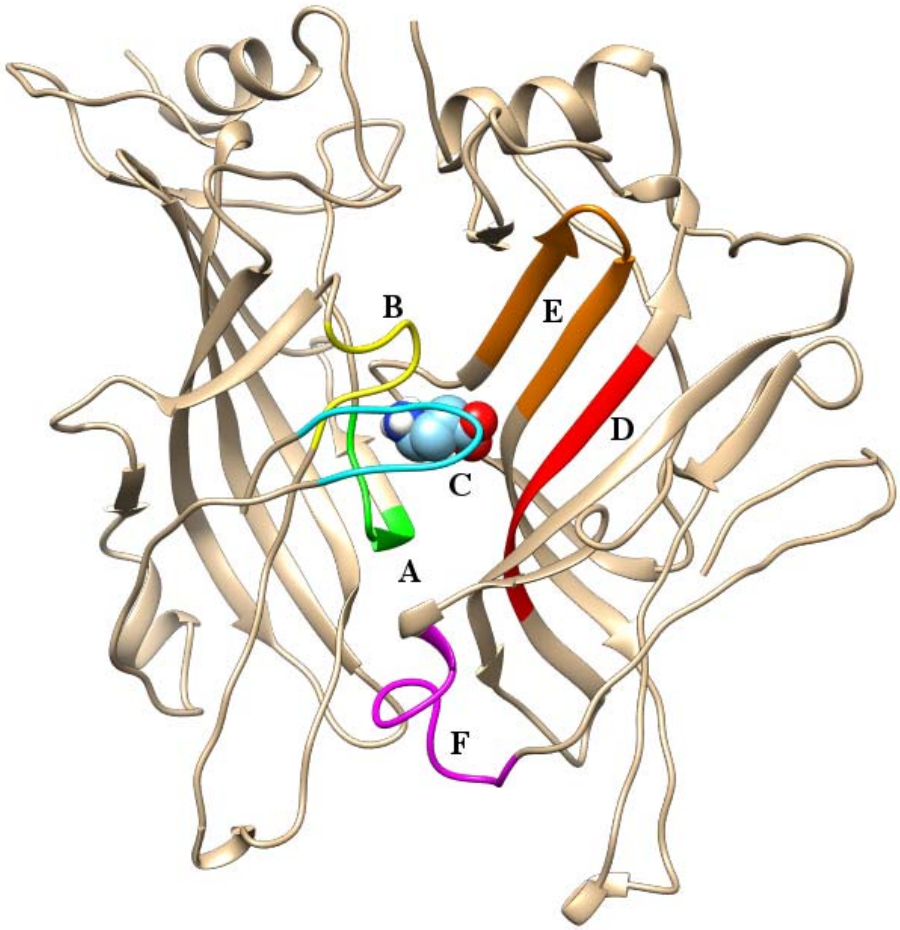

Figure 6: A model of the GABA binding site found between adjacent subunits of the *H. contortus* UNC-49 receptor. Labels indicate principle (A-C) and complimentary (D-F) loops.

1.12 Key Tools for Ion Channel Research

There are a variety of methods that can be utilized for ion channel research, from the characterization of individual amino acid residues to the analysis of more complex intermolecular interactions for their impact on channel function. Some methods are able to provide more detail to supplement static imaging (such as X-ray crystallography) and allow the channel to be analyzed before, during, and after activation. Some of the methods utilized for this thesis are described in the following sections.

1.13 *Xenopus laevis* Expression System

The oocytes of the African Clawed frog, *Xenopus laevis*, have been used as a means of translating foreign mRNA into functional proteins since the early 70s (Gurdon et al., 1971). It was discovered that *X. laevis* oocytes are able to translate a wide variety of mRNA from bacteria, plants, and animals while maintaining a high level of translation efficiency over extended periods of time (Gurdon et al., 1971; Sobczak et al., 2010). Another benefit of this system is the large size of the oocytes, with a diameter of between 1-1.3 mm making them easy to isolate and work with, such as for performing microinjections (Sobczak et al., 2010). The durability of the oocytes' membrane and their large size also permits the use of two-electrode voltage clamp (TEVC) electrophysiology, which has been shown to be more accurate than other recording methods for cells that are too small for TEVC recording (Sherman-Gold, 1993). The oocytes have been shown to be viable for microinjection of mRNA and electrophysiology recording for at least 3 weeks following surgical extraction, demonstrating their durability in an experimental setting.

1.14 Mutant Cycle Analysis

One method that can be utilized to identify and measure intermolecular interactions between residues in proteins of a known structure is mutant cycling (Horovitz, 1996). These experiments require three separate mutations in order to determine the strength of interactions between two residues. Specifically, it requires the wild-type protein, two single mutants, and a double mutant containing both mutations simultaneously (Horovitz, 1996). Although the method was initially used in the early 1980's for protein engineering of tyrosyl-tRNA synthetase (Carter, 1984), it has since

been found to have other useful applications. The information obtained from proteins with known structures can be useful in determining structural details for proteins where the structure is not known. It can provide structural information for ligand-bound proteins relating to transition states during binding, such as GABA molecules bound to LGICs (Horovitz, 1996). The mutations for mutant cycle analysis are conducted with alanine residues whenever possible to prevent new interactions from being formed when other mutations are implemented (Horovitz, 1996). The formula for calculating the change in free energy of a mutation compared to the wildtype (Venkatachalan & Czajkowski, 2008) is as follows:

$$\Delta G = RT\ln\left(\frac{\text{mut } EC_{50}}{\text{wt } EC_{50}}\right)$$

Where ΔG is the change in free energy, R is the ideal gas constant, T is the temperature, mut EC_{50} is the half-maximal response of the ligand in the mutant protein, and wt EC_{50} is the half-maximal response of the ligand in the wildtype protein. To calculate the overall interaction energy between two residues (Venkatachalan & Szajkowski, 2008), the following equation is used:

$$\Delta\Delta G = RT\ln\left(\frac{(\text{mut1,2 } EC_{50})(\text{wt } EC_{50})}{(\text{mut1 } EC_{50})(\text{mut2 } EC_{50})}\right)$$

Where $\Delta\Delta G$ is the overall interaction energy, R is the ideal gas constant, T is the temperature, mut1 EC_{50} is the half-maximal response of first mutation, mut2 EC_{50} is the half-maximal response of second mutation, mut1,2 EC_{50} is the half-maximal response of the double mutation, and wt EC_{50} is the half-maximal response of the wildtype protein. When a double mutation displays the combined effect of the two corresponding single

mutants (such that $\Delta\Delta G = 0$), the mutations are thought to have an additive effect on the protein (Horovitz, 1996). A value of $\Delta\Delta G \neq 0$ implies that the combined effect of both mutations are non-additive and the two residues in question interact with each other in some way (Venkatachalan & Czajkowski, 2008).

1.15 Disulfide Trapping

Disulfide trapping is a method that can be utilized to determine spatial proximity between two potentially interacting residues in an LGIC and to determine what impact those residues have, if any, on ligand binding and channel activation (Venkatachalan & Czajkowski, 2008). It is conducted by mutating each residue in question to a cysteine and cross-linking the two cysteine residues together using the oxidizing agent, hydrogen peroxide (H_2O_2), to form a strong disulfide bond (Venkatachalan & Czajkowski, 2008). Electrophysiology is conducted before and after cross-linking, and agonist binding response using the appropriate EC_{50} concentrations are recorded to measure the effect of the disulfide bond on the channel. Finally, the disulfide reducing agent dithiothreitol (DTT) is used to restore the channel to the initial mutated state and agonist binding is measured again (Venkatachalan & Czajkowski, 2008). Double cysteine mutations within the agonist binding pocket may display reduced agonist response when exposed to H_2O_2 due to proximal interference with the ligand. As an example, a disulfide trapping experiment was conducted on the β subunit of the $GABA_A$ receptor which analyzed highly conserved potentially interacting residues thought to be critical for GABA activation. It was found that E153 and K196 in the $GABA_A$ receptor form a salt bridge that is important for regulating loop C movement during GABA binding, allowing the channel to enter the open state (Venkatachalan & Czajkowski, 2008). The E153 residue

of the $GABA_A$ receptor is analogous to E183 in the Hco-UNC-49 receptor. K196 in the $GABA_A$ receptor does not have an analogous counterpart in invertebrates, but sequence homology has revealed that several invertebrate GABA receptors have a highly conserved threonine in that position (Figure 7 in methods section). This may attribute to some functional differences that make the invertebrate receptor unique compared to its vertebrate counterpart.

1.16 Objectives of this Thesis

There is good evidence that the UNC-49 GABA receptor of *H. contortus* can be developed into a future antiparasitic drug target (Accardi et al., 2012). However, any development of new drugs targeting this receptor will require a detailed understanding of the structural components that are important for ligand-binding and channel function. Important intermolecular interactions play a crucial role in determining a protein's structure and function. This thesis aims to analyze the intermolecular interactions of residues found in the *H. contortus* UNC-49 GABA receptor that are not conserved among vertebrates. This will lead to a better understanding of how these parasite receptors function and provide insight to future researchers for the development of novel anthelmintics.

Methods

Section 2: Methods

2.1 Hco-UNC-49 Channel Modelling

A *C. elegans* GluCl channel was used as a template to generate the *H. contortus* UNC-49 model (Kaji et al., 2015) (Figure 6) and was used to initially analyze amino acid proximity between residues of interest. USCF Chimera 1.11, developed by the Resource for Biocomputing, Visualization, and Informatics (RBVI) at the University of California (La Jolla, CA, United States) was used to analyze and manipulate the model and identify bond lengths.

2.2 Hco-UNC-49B Primer design

Point mutations were determined based on the position of charged amino acids conserved among nematodes within the full-length sequence of Hco-UNC-49B (GenBank, Accession #: ACL14329). This sequence was aligned with a variety of other GABA receptors from humans, *C. elegans*, *Drosophila melanogaster*, *Brugia malayi*, *Trichinella pseudospiralis*, and *Toxocara canis* (Figure 7). Mutant primers were generated using the QuikChange Primer Design program from Agilent Technologies (www.genomics.agilent.com/primerDesignProgram.jsp) to ensure full compatibility with the QuikChange II Mutagenesis Kit. Custom DNA oligos were ordered from Integrated DNA Technologies.

Initial mutations were designed to replace single charged amino acid residues with an uncharged alanine or a residue of the opposite charge (such as lysine to glutamic acid) to measure the impact of that specific point mutation. Further mutations allowed key residues to have their charges swapped to check for potential salt bridge restoration

(if one is present), or to nullify the charge on both sides of an interacting pair simultaneously. The full list of primers utilized can be found in Table 1.

Table 1: Primers utilized for mutagenesis of Hco-UNC-49B.

Mutant	Forward Primer	Reverse Primer
D83C	5'-GCCATGTTTGTCGCATATAGAAAC ATAGCGTAAAGTCCATATCCACTT-3'	5'-AAGTGGATATGGACTTTACGCTAT GTTTCTATATGCGACAAACATGGC-3'
D83N	5'-CATGTTTGTCGCATATAGAAATTT AGCGTAAAGTCCATATCCACT-3'	5'-AGTGGATATGGACTTTACGCTAAA TTTCTATATGCGACAAACATG-3'
E131A	5'-GTGGAAAAACGATTTCTTCGCGTT CGGGAAAAACGTATC-3'	5'-GATACGTTTTTCCCGAACGCGAAG AAATCGTTTTTCCAC-3'
E131C	5'-CCAAGTGGAAAAACGATTTCTTGC AGTTCGGGAAAAACGTATCCGGC-3'	5'-GCCGGATACGTTTTTCCCGAACTG CAAGAAATCGTTTTTCCACTTGG-3'
K181A	5'-CAATAGCTTTCAATTTCCAGCGCGC ATCGTTGTGAATCCATCGG-3'	5'-CCGATGGATTCACAACGATGCGCG CTGGAAATTGAAAGCTATTG-3'
K181C	5'-GCAATAGCTTTCAATTTCCAGGCA GCATCGTTGTGAATCCATCGG-3'	5'-CCGATGGATTCACAACGATGCTGC CTGGAAATTGAAAGCTATTGC-3'
K181E	5'-TAGCTTTCAATTTCCAGCTCGCAT CGTTGTGAATCCATC-3'	5'-GATGGATTCACAACGATGCGAGC TGGAAATTGAAAGCTA-3'
K181R	5'-TTTCAATTTCCAGCCTGCATCGTTG TGAATCCATCGG -3'	5'-CCGATGGATTCACAACGATGCAG GCTGGAAATTGAAA -3'
K181T	5'-TAGCTTTCAATTTCCAGCGTGCATC GTTGTGAATCCATC-3'	5'-GATGGATTCACAACGATGCACGC TGGAAATTGAAAGCTA-3'
E183A	5'-GTATAGCAATAGCTTTCAATTGCCA GCTTGCATCGTTGTGAAT-3'	5'-ATTCACAACGATGCAAGCTGGCAA TTGAAAGCTATTGCTATAC-3'
E183C	5'-CCATTGTATAGCAATAGCTTTCAAT GCACAGCTTGCATCGTTGTGAATCCAT C-3'	5'-GATGGATTCACAACGATGCAAGC TGTGCATTGAAAGCTATTGCTATACA ATGG-3'
E183D	5'-GTATAGCAATAGCTTTCAATATCCA GCTTGCATCGTTGTGA-3'	5'-TCACAACGATGCAAGCTGGATAT TGAAAGCTATTGCTATAC-3'
E183K	5'-TGTATAGCAATAGCTTTCAATTTTC AGCTTGCATCGTTGTGAATCC-3'	5'-GGATTCACAACGATGCAAGCTGA AAATTGAAAGCTATTGCTATACA-3'
T230K	5'-GATGTGGTTGCTTGTTTGTAATTTA CATGATAGCAAGTCTGCTTG-3'	5'-CAAGCAGACTTGCTATCATGTAAA TTACAAACAAGCAACCACATC-3'
K181A-E183A	5'-GCCATAGCTTTCAATTGCCAGCGC GCATCGTTG-3'	5'-CAACGATGCGCGCTGGCAATTGA AAGCTATGGC-3'
K181C-E183C	5'-CCATTGTATAGCAATAGCTTTCAAT GCACAGGCAGCATCGTTGTGAATCCA TC-3'	5'-GATGGATTCACAACGATGCTGCCT GTGCATTGAAAGCTATTGCTATACAA TGG-3'
K181E-E183K	5'-TGTATAGCAATAGCTTTCAATCTCC AGTTTGCATCGTTGTGAATCCATC-3'	5'-GATGGATTCACAACGATGCAAAC TGGAGATTGAAAGCTATTGCTATAC A-3'

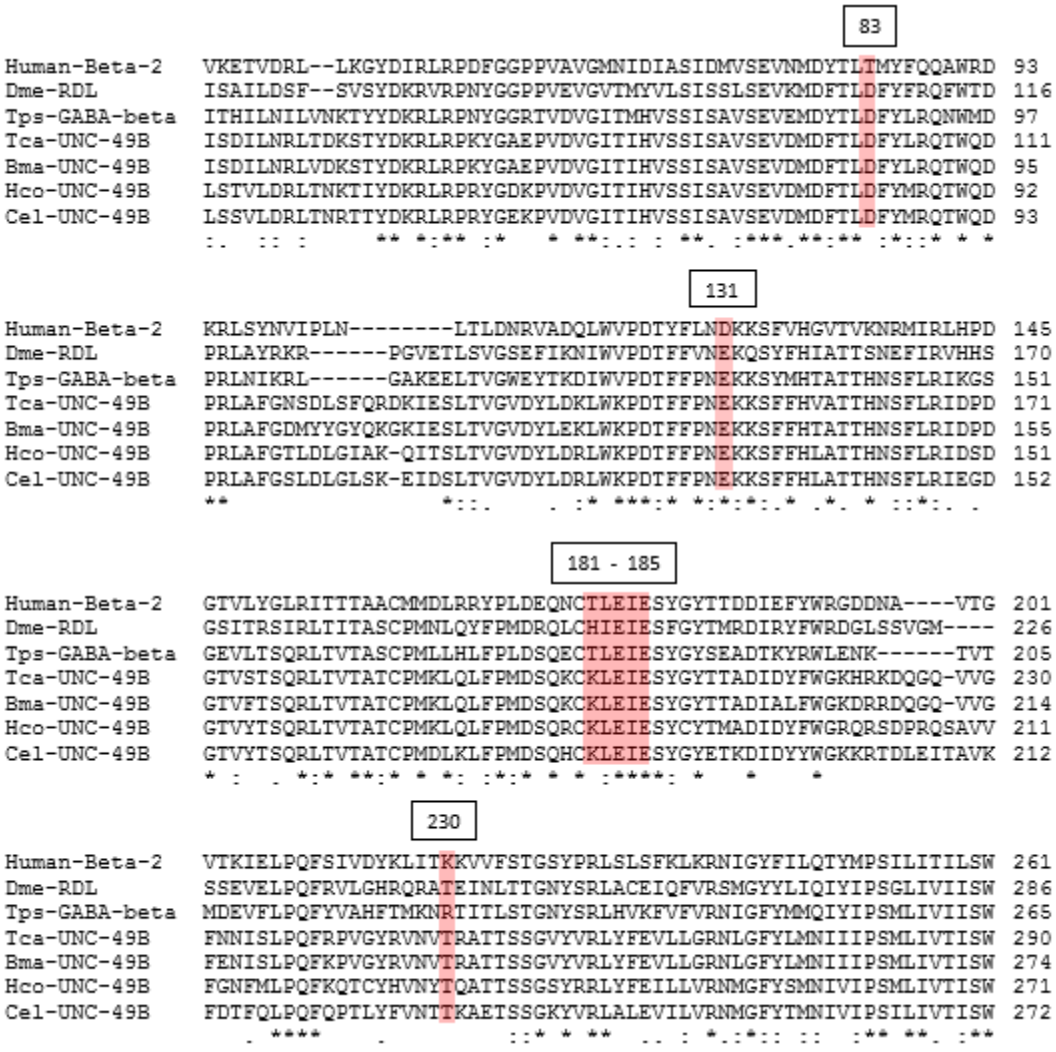

Figure 7: Sequence alignment of Hco-UNC-49B with other GABA channels. Highlighted areas represent residues being modified within Hco-UNC-49B for this thesis. GABA receptor subunit sequences include (from top to bottom) human, *D. melanogaster*, *T. pseudospiralis*, *T. canis*, *B. malayi*, *H. contortus*, and *C. elegans*.

2.3 Site Directed Mutagenesis and cRNA Synthesis

McGill University provided the mRNA initially required to produce the coding sequence for Hco-UNC-49B. The sequence was cloned into the pT7TS vector, nested within an untranslated *Xenopus laevis* beta-globin gene to allow expression within the oocyte model. Point mutations were performed via PCR utilizing the previously

mentioned primers and the QuikChange II Mutagenesis Kit (Agilent Technologies, Santa Clara, CA, United States). Mutant DNA was then transformed into supercompetent *E. coli* cells, which were then amplified on ampicillin agarose plates, and further grown in ampicillin LB broth. Plasmids were isolated using the EZ-10 Spin Column Plasmid DNA Minipreps Kit (Bio Basic, Ontario, Canada) and sequences were confirmed via offsite sequence analysis at McGill University (Genome Quebec). *In vitro* cRNA synthesis was conducted using the mMESSAGE mMACHINE T7 Transcription Kit (Ambion, Austin, TX, United States). Following transcription and addition of DNase, cRNA was precipitated with lithium chloride, washed with ethanol, and re-suspended in nuclease-free water.

2.4 Surgical Extraction of *X. laevis* Oocytes

Female *Xenopus laevis* frogs obtained from Nasco (Nasco, Fort Atkinson, WI, United States) were anaesthetized via a short bath in 0.15% ethyl 3-aminobenzoate methanesulfonate solution (MS-222; Sigma-Aldrich, Oakville, Ontario, Canada) using sodium bicarbonate to reach pH 7. Lobes of the ovary were surgically extracted through a small incision on the left or right side of the torso, further separated into smaller fragments, and defolliculated at room temperature on a rocker in a mixture of collagenase (1 mL, 10 mg/mL; Sigma-Aldrich) and OR-2 (4 mL; 82 mM NaCl, 2 mM KCl, 1 mM $MgCl_2$, 5 mM HEPES). Oocytes were stored in an incubator at 18.5°C in a supplemented ND96 solution (96 mM NaCl, 2 mM KCl, 1.8 mM $CaCl_2$, 1 mM $MgCl_2$, 5 mM HEPES, 0.5 mM gentamycin, 0.275 ug/mL sodium pyruvate) until ready for use.

X. laevis frogs were stored in a climate-controlled room in large tanks containing conditioned water with a maximum of 3 frogs per tank. One extra tank was used solely

for surgical recovery, with a reduced water level allowing for easy surface access by post-surgery frogs. Each frog was fed 1g of Nasco frog brittle (Nasco, Fort Atkinson, WI, United States) twice weekly, and tanks were cleaned and water-cycled on each day following feeding. Day-night cycles were artificially controlled on a timer to mimic natural conditions and the room was checked daily.

2.5 TEVC Electrophysiology on *X. laevis* Oocytes

Selected *X. laevis* oocytes were injected with a 50 nL mixture containing equal parts *unc-49b* (mutant or wildtype) and wildtype *unc-49c* cRNA using a Drummond Nanoject II microinjector (Drummond Scientific Company, Broomhall, PA, United States) attached to a micromanipulator (World Precision Instruments, Sarasota, FL, United States). Needles for injections were pulled from glass capillaries (Harvard Apparatus, Holliston, MA, United States) using the P-97 Flaming/Brown Micropipette Puller (Sutter Instruments Co., Novato, CA, United States). Oocytes were then placed back into an 18.5°C incubator for at least 2 days to allow membrane receptor expression to occur. Supplemented ND96 solution was changed at least once each day following injections until electrophysiology was conducted.

The two-electrode voltage clamp (TEVC) method was utilized to monitor channel activity of the UNC-49 GABA receptor. Electrophysiology was performed 2 days post-injection using the Axoclamp 900A voltage clamp (Molecular Devices, Sunnyvale, CA, United States). Electrodes pulled from glass capillaries using the P-97 Micropipette Puller were filled with 3M KCl and connected to an appropriate Axon Instrument Headstage (Molecular Devices) with a small silver wire. Injected oocytes were pierced with two electrodes, one to clamp the voltage of the oocyte at a constant -60 mV and the

second to record any changes in current that can occur during channel activation (Figure 8). Oocytes were constantly washed with non-supplemented ND96 solution (96 mM NaCl, 2 mM KCl, 1.8 mM $CaCl_2$, 1 mM $MgCl_2$, 5 mM HEPES) between application of other compounds. Perfusion of solution across the oocytes was performed using the RC-1Z perfusion chamber (Warner Instruments, Holliston, MA, United States) and a Fisherbrand Variable-Flow Peristaltic Pump (Fisher Scientific, Hampton, NH, United States) to remove waste liquid.

Electrophysiological traces from individual oocytes were analyzed for the change in current following a channel response at each test concentration. Dose-response curves were then generated using GraphPad Prism (GraphPad Software, San Diego, CA, United States) with data being fitted to the following formula:

$$I_{max} = \frac{1}{1 + \left(\frac{\mathrm{EC}_{50}}{[D]}\right)^{h}}$$

For this formula, I_{max} corresponds to the maximal response, EC_{50} is the concentration of the agonist that produces 50% of the maximal response, [*D*] is the concentration of that agonist, and *h* is the Hill coefficient.

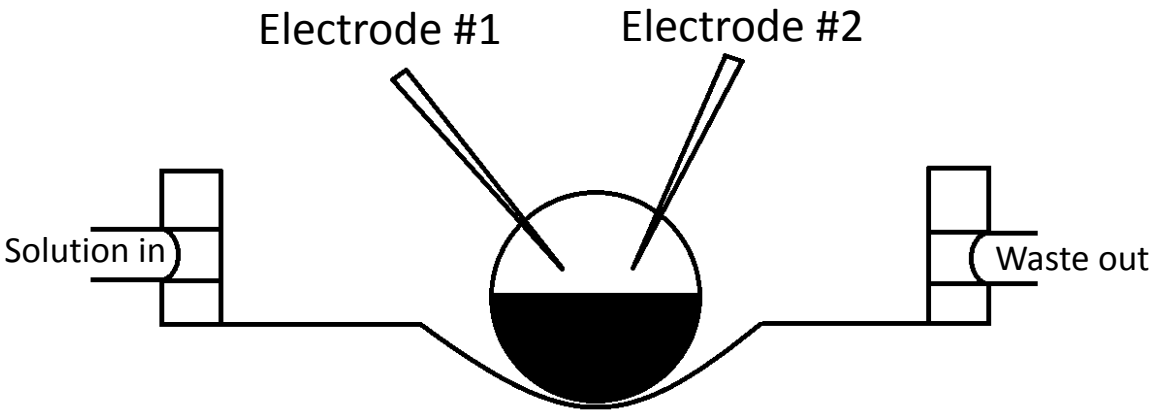

Figure 8: A *Xenopus laevis* oocyte set up for two-electrode voltage clamp electrophysiology in a perfusion chamber.

2.6 Disulfide Trapping

Disulfide trapping experiments were conducted on cysteine mutations of UNC-49B (K181C, E183C, and a double cysteine mutant) to determine their ability to interact with each other and their effect on ligand binding and activation of the channel. A strong disulfide bond between mutated cysteine residues introduced by exposure to H_2O_2 can result in reduced channel agonist sensitivity, which can be restored via exposure to DTT. TEVC electrophysiology was utilized to record the response of each mutant to the calculated EC_{50} GABA concentration before and after cysteine cross-linking (disulfide bond formation) had occurred. After retrieving a baseline response via GABA perfusion, oocytes were washed with ND96 until a stable current was achieved, at which point a 0.3% H_2O_2 solution was perfused over the oocytes for 1 minute to induce disulfide bond formation in the receptor. H_2O_2 was diluted with ND96 buffer from a 30% H_2O_2 stock solution (Sigma-Aldrich, Oakville, Ontario, Canada) to reach the desired 0.3%. Another ND96 wash was conducted until a stable current was achieved, and response to the corresponding EC_{50} GABA concentration was recorded. An ND96 wash was once again

repeated for current stabilization followed by a 1-minute perfusion of 10mM DTT (Sigma-Aldrich, Oakville, Ontario, Canada) diluted in ND96 buffer to remove the disulfide bond formed by H_2O_2 exposure. A final EC_{50} GABA response was recorded upon current stabilization following DTT exposure.

2.7 Agonists and Other Compounds Utilized for Electrophysiology

GABA agonists used for this research were (R)-(-)-4-Amino-3-hydroxybutyric acid (R-GABOB), (S)-(+)-4-Amino-3-hydroxybutyric acid (S-GABOB), Imidazole-4-acetic acid (IMA), and 5-aminovaleric acid (DAVA). R-GABOB was obtained from Astatech (Astatech Inc., Bristol, PA, United States). All other agonists were obtained from Sigma (Sigma-Aldrich, St. Louis, MO, United States). Electrophysiology on *X. laevis* oocytes expressing mutant or wildtype Hco-UNC-49BC receptors was conducted by first exposing the oocyte to the corresponding EC_{50} GABA concentration to ensure channel functionality. Following this, a range of increasing concentrations for the agonist being tested were washed over the egg and changes in current across the membrane were recorded. Dose response curves were generated using this range of recordings. Concentration range for DAVA was between 250µM and 50000µM since it has been shown to be only a partial agonist for GABA (Kaji et al., 2015). All other agonist concentrations ranged from 50µM to 10000µM.

The negative allosteric modulator (NAM) of GABA receptors used in this research, pregnenolone sulfate (PS), was obtained from Sigma (Sigma-Aldrich, St. Louis, MO, United States). *X. laevis* oocytes expressing mutant or wildtype Hco-UNC-49BC receptors were first exposed to EC_{50} concentrations of GABA to ensure channel functionality. Oocytes were then exposed to a co-application of an increasing range of PS

concentrations mixed with the corresponding EC_{50} GABA concentration. Changes in current were recorded and inhibitory dose response curves were generated to determine the IC_{50} value for the mutant being tested. PS concentrations ranged from 5μM to 500μM.

Results

Section 3: Results

3.1 Electrophysiology of Hco-UNC-49

Point mutations were conducted within the UNC-49B subunit of the UNC-49 GABA receptor to determine the importance of individual amino acid residues. The residues located at D83, E131, K181, E183, and T230 positions within UNC-49B were changed to several other residues to monitor the resulting changes in channel activation. Each EC_{50} value is the result of a minimum of 4 recorded traces from *X. laevis* oocytes of at least 2 different frogs. Some mutations in the K181 position resulted in minimal change to EC_{50} values, while all mutations in the E183 position caused a drastic decrease in GABA sensitivity. EC_{50} values for key mutations have been rank ordered and are shown in Figure 9. A summary of all EC_{50} results is displayed in Table 2.

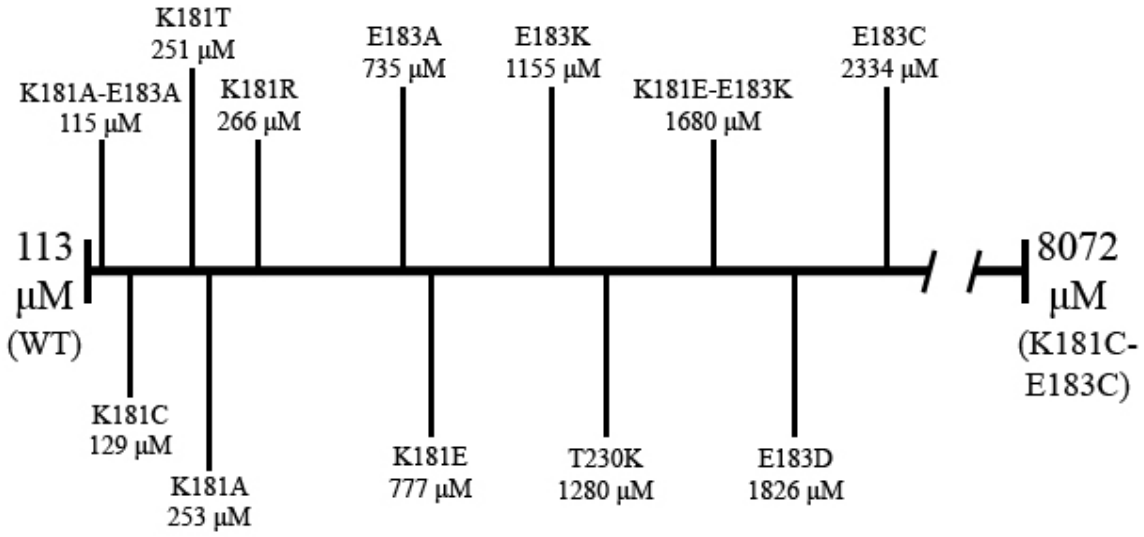

Figure 9: A visualization of increasing EC_{50} values for mutations in K181, E183, and T230 of Hco-UNC-49B.

Table 2: EC_{50} values and number of oocytes tested for a variety of mutations in Hco-UNC-49B.

Mutant	**EC_{50} ± Standard Error (μM)**	**Hill Slope**	**Number of Oocytes**
Wildtype UNC-49B/C	113 ± 10.83	1.54	15
D83A*	No Response <20 mM	-	10
D83C	578.5 ± 116.59	1.05	10
D83E*	276.1 ± 36.99	2.06	5
D83N	335.1 ± 48.90	1.71	9
E131A	219.1 ± 20.61	0.88	5
E131C	1054 ± 210.41	1.07	11
K181A	252.9 ± 40.72	1.22	9
K181C	128.8 ± 10.32	1.22	12
K181E	776.7 ± 38.03	2.35	11
K181R	265.6 ± 59.01	1.12	5
K181T	251.3 ± 26.64	1.63	10
E183A*	735.2 ± 131.48	1.42	6
E183C	2334 ± 318.49	0.97	12
E183D	1826 ± 282.69	1.26	6
E183K	1155 ± 77.66	2.70	13
T230K	1280 ± 118.46	1.31	12
K181A-E183A	114.7 ± 7.48	2.73	8
K181C-E183C	8072 ± 582.26	2.30	16
K181E-E183K	1680 ± 276.98	0.99	13
K181T-T230K	No Response <20 mM	-	9

*Data obtained from Josh Foster included to provide context

3.2 K181 Mutations

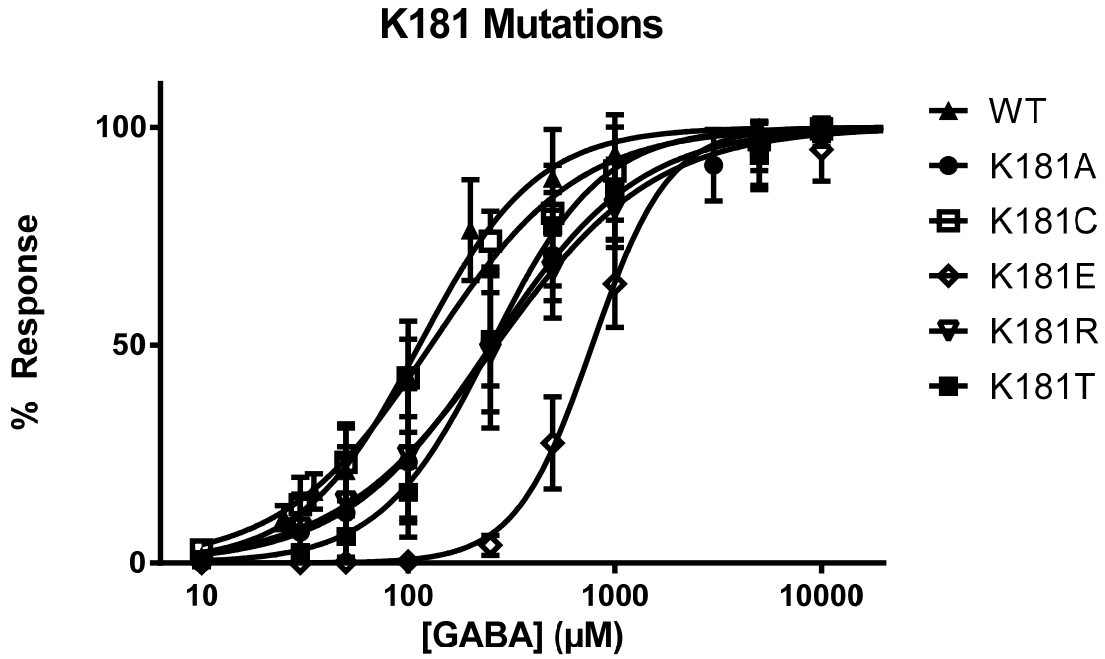

Figure 10: Dose response curves for mutations of Hco-UNC-49B at the K181 position.

The K181 position was selected as a residue of interest based on its charge and proximity to an oppositely charge residue (E183) with which a potential salt bridge could be formed. The first mutation to remove any charge present from the K181 position was a mutation from lysine to alanine. This mutation showed an EC_{50} of 252.9μM ± 40.72 (n=9). The next step was to reverse the charge via a K181E mutation, which showed a greater reduction (approximately 7-fold) in GABA sensitivity with an EC_{50} of 776.7μM ± 38.03 (n=11). Mutating K181 to a similarly charged arginine (K181R) resulted in an over 2-fold reduction in GABA sensitivity with an EC_{50} of 265.6μM ± 59.01 (n=5). The lysine to cysteine mutation (K181C) displayed no significant change in GABA response compared to wildtype with an EC_{50} of 128.8μM ± 10.32 (n=12). Modification of K181 to a threonine was conducted for two reasons. First to test if polarity (as opposed to electric

charge) had an impact on the channel at this position, and secondly because a threonine is present in the analogous position in the human GABA receptor. The K181T mutation showed an over 2-fold decrease in GABA sensitivity with an EC_{50} of 251.3µM ± 26.64 (n=10). Dose response curves for all K181 single mutations can be seen in Figure 10.

3.3 E183 Mutations

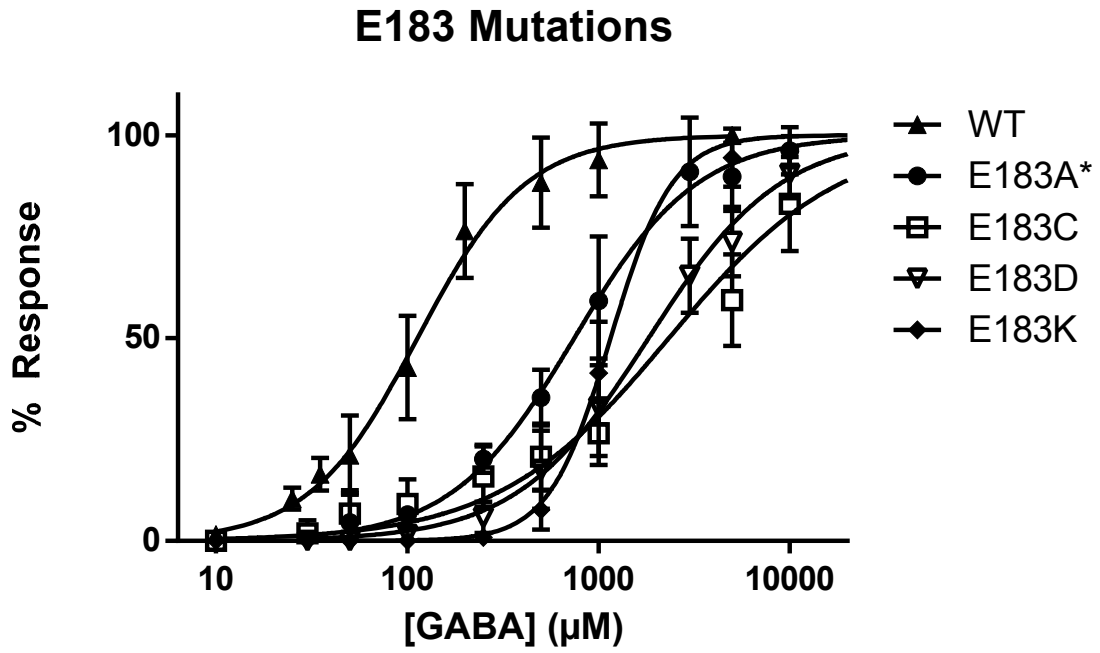

Figure 11: Dose response curves for mutations of Hco-UNC-49B at the E183 position. *Data obtained from Josh Foster

Mutations in the E183 position were conducted to investigate the second half of a potential salt bridge between K181 and E183. The initial mutation of E183A to determine the effect of removing the negatively charged glutamic acid showed an EC_{50} of 735.2µM ± 131.48 (n=6), which is a 6.5-fold decrease in GABA sensitivity. Reversing the charge at E183 via a mutation to lysine (E183K) displayed a greater than 10-fold reduced GABA response with an EC_{50} of 1155µM ± 77.66 (n=13). The E183D mutation was conducted

to measure the effect of replacing glutamic acid with an equally negatively charged, but smaller amino acid, and resulted in a drastic decrease in GABA sensitivity (a 16-fold reduction) with an EC_{50} of 1826μM ± 282.69 (n=6). Mutation to a cysteine at the E183 position also resulted in a large (over 20-fold) decrease in GABA sensitivity with an EC_{50} of 2334μM ± 318.49 (n=12). Dose responses for E183 single mutations can be found in Figure 11.

3.4 K181-E183 Charge Reversal Mutation

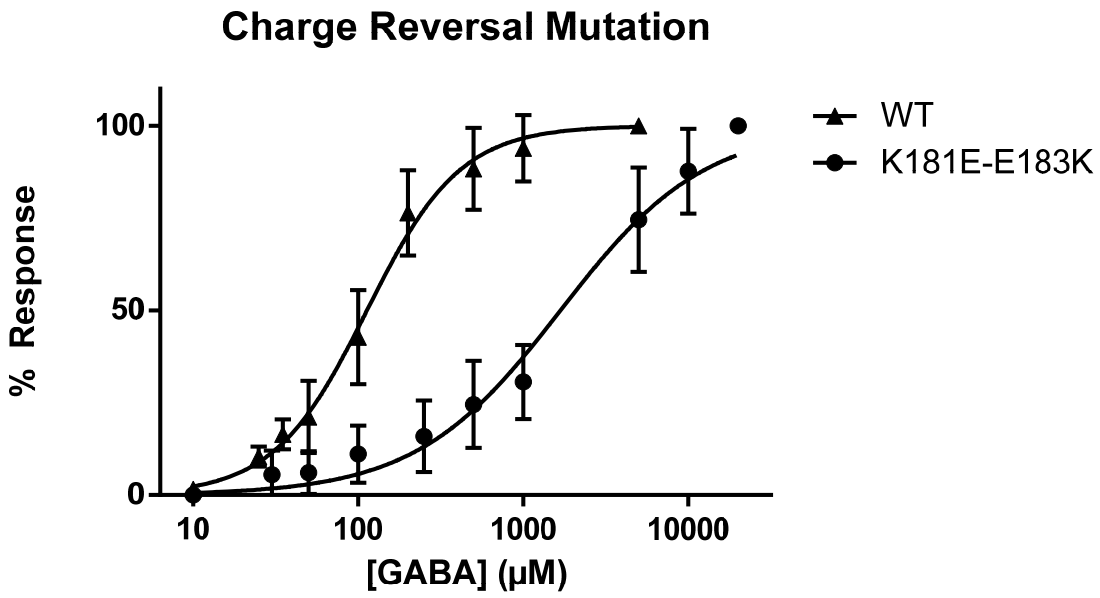

Figure 12: Dose response curve for the charge reversal mutation of Hco-UNC-49B at the K181 and E183 positions.

In order to determine the potential presence of a salt bridge between the K181 and E183 residues, a double mutation in which the residues (and therefore the electrical charge) on either side of the bridge has been swapped is required. For this mutation, lysine at 181 is mutated to a glutamic acid while the glutamic acid at 183 is simultaneously mutated to a lysine. This mutation resulted in a large decrease,

approximately 15-fold, in GABA sensitivity with an EC_{50} of 1680µM ± 276.98 (n=13). The dose response for this can be seen in Figure 12.

3.5 K181-E183 Charge Removal Mutation

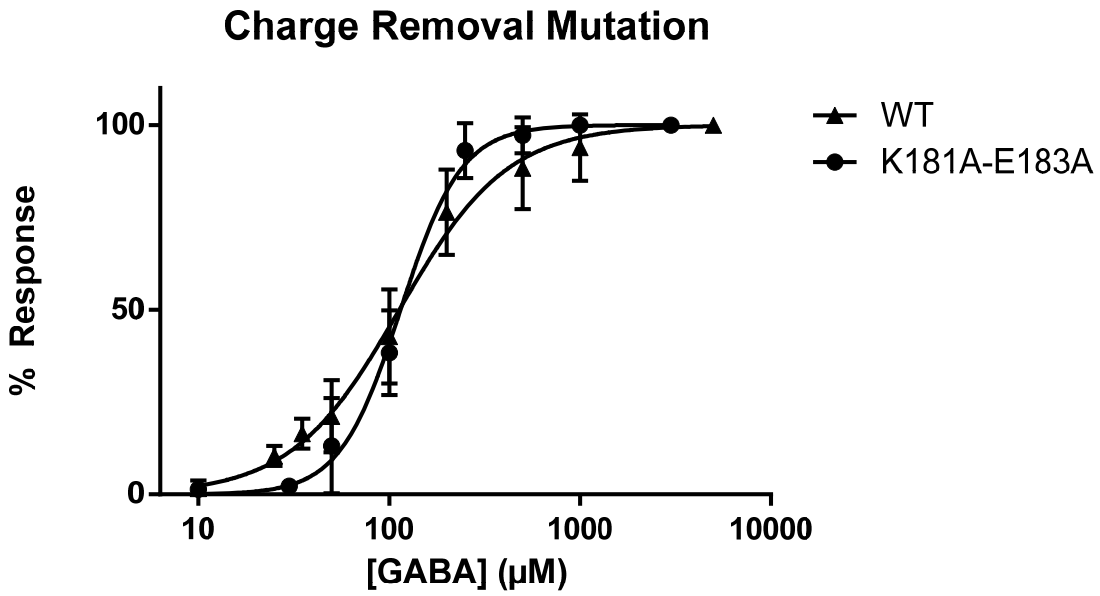

Figure 13: Dose response curve for the double charge removal mutation of Hco-UNC-49B at the K181 and E183 positions.

To determine the impact of removing all charges from the two potentially interacting residues at the K181 and E183 positions, a double alanine mutation was created. Based on the previous results from the K181A and E183A mutations, it was expected that a double alanine mutation would have a greater reduction in GABA sensitivity due to the combined effect of removing both charges simultaneously. Surprisingly, the double alanine mutation resulted in an EC_{50} of 114.7µM ± 7.48 (n=8), which closely resembled the wildtype EC_{50} of 113µM. The hill slope of the double alanine mutant (2.73) was found to be significantly different from the wildtype (1.54) hill slope ($p<0.05$). The dose response for this mutation can be seen in Figure 13.

3.6 K181-T230 Mutations

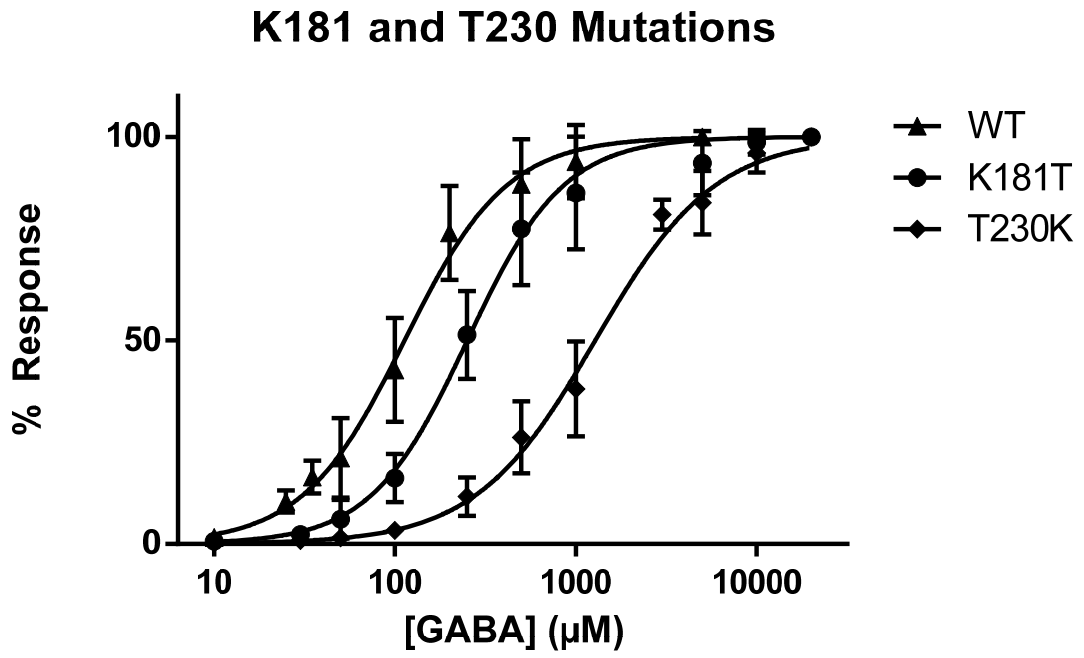

Figure 14: Dose response curves for mutations of Hco-UNC-49B at the K181 (n=10) and T230 (n=12) positions.

The threonine in the 230 position and the lysine in the 181 position were both found to be conserved among a variety of parasitic nematodes after a sequence alignment was conducted (Figure 7). Interestingly, in the human β-2 $GABA_A$ receptor, there is a lysine in the 230 position and a threonine in the 181 position. To determine if the placement of these two residues is critical for receptor function in *H. contortus*, a series of mutations were conducted. The results for K181T have been presented in a previous subsection. The mutation of T230 to a lysine resulted in a large, over 11-fold decrease in GABA sensitivity with an EC_{50} of 1280μM ± 118.46 (n=12). The swap mutation replacing K181 with a threonine and T230 with a lysine simultaneously did not respond

to any GABA concentrations below 20 mM and is therefore considered to be effectively non-functional. The dose response curves for these mutations can found in Figure 14.

3.7 GABA Agonists and Other Compounds

Since the results from the K181A and K181A-E183A were unexpected, further testing was conducted utilizing multiple GABA agonists to better characterize the Hco-UNC-49 receptor. Testing on the K181A mutation included electrophysiological responses to the GABA receptor agonists (S)-(+)-4-Amino-3-hydroxybutyric acid (S-GABOB), (R)-(-)-4-Amino-3-hydroxybutyric acid (R-GABOB), and Imidazole-4-acetic acid (IMA). Testing on the K181A-E183A mutation included the GABA receptor agonists IMA and 5-aminovaleric acid (DAVA), and the GABA receptor NAM pregnenolone sulfate (PS). Previous work in this lab characterized the wildtype Hco-UNC-49 receptor using the aforementioned compounds and are presented for comparison (Kaji et al., 2015). Results for these compounds are summarized in Table 3.

For the K181A mutation, S-GABOB yielded an EC_{50} of 2111µM ± 194.69 (n=7), a 5.5-fold decrease in channel sensitivity compared to the wildtype receptor with S-GABOB, and an 8-fold decrease in sensitivity compared to GABA. R-GABOB had an EC_{50} of 1101µM ± 138.74 (n=5), a nearly 5-fold decrease compared to the wildtype receptor, and an over 4-fold decrease compared to GABA. IMA had an EC_{50} of 208.1µM ± 18.74 (n=4), a similar channel sensitivity compared to wildtype and a slight increase compared to GABA. Dose response curves can be seen in Figure 15.

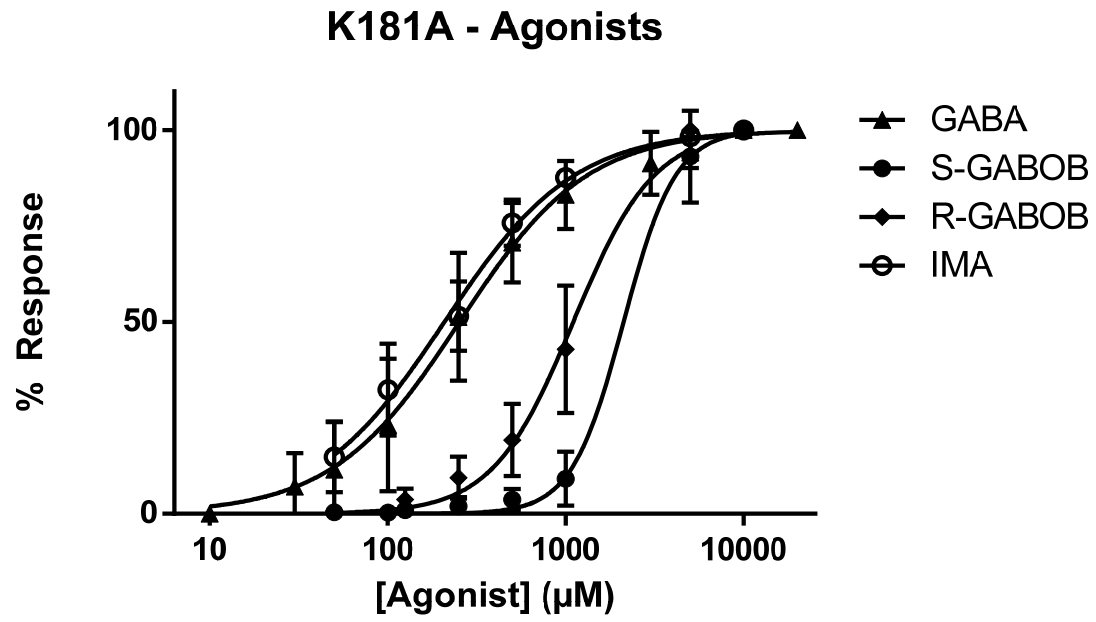

Figure 15: Dose response curves for agonists tested on the K181A mutation of Hco-UNC-49B.

With the double alanine mutation, K181A-E183A, IMA had an EC_{50} of 207.2µM ± 30.38 (n=4), nearly the same as the wildtype receptor, and about a 2-fold decrease compared to GABA. DAVA yielded an EC_{50} of 3429µM ± 400.3 (n=4), which is very close to the wildtype receptor and is a 30-fold decrease when compared to GABA. Agonist response curves can be seen in Figure 16. The GABA receptor NAM, PS, had an IC_{50} of 65.25µM ± 24.58 (n=6) which is a nearly 2.5-fold decrease in inhibitory effect when compared to the wildtype IC_{50} of 26.83 ± 0.39 (n=5). PS response curves can be seen in Figure 17.

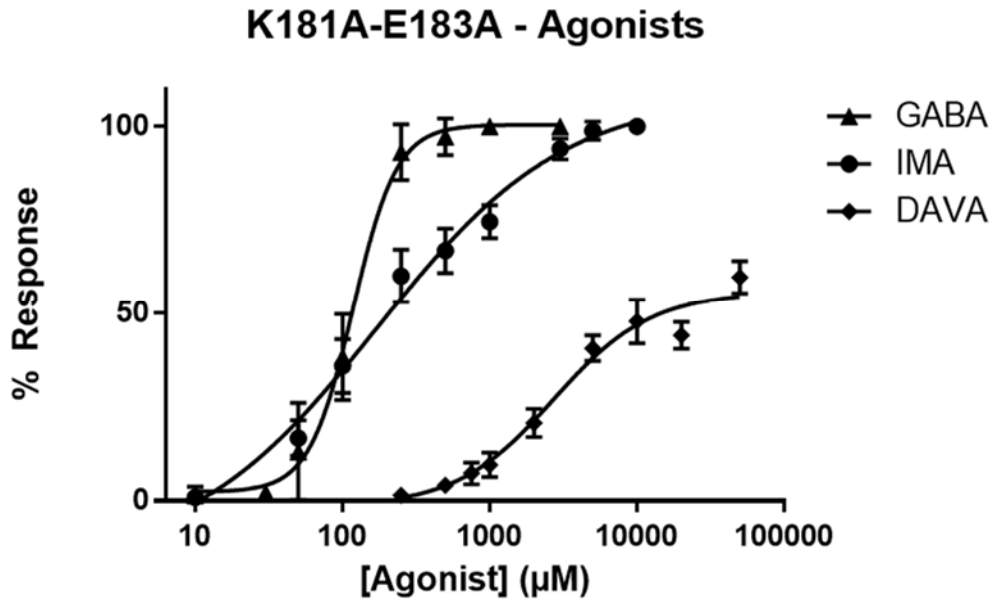

Figure 16: Dose response curves for agonists tested on the K181A-E183A mutation.

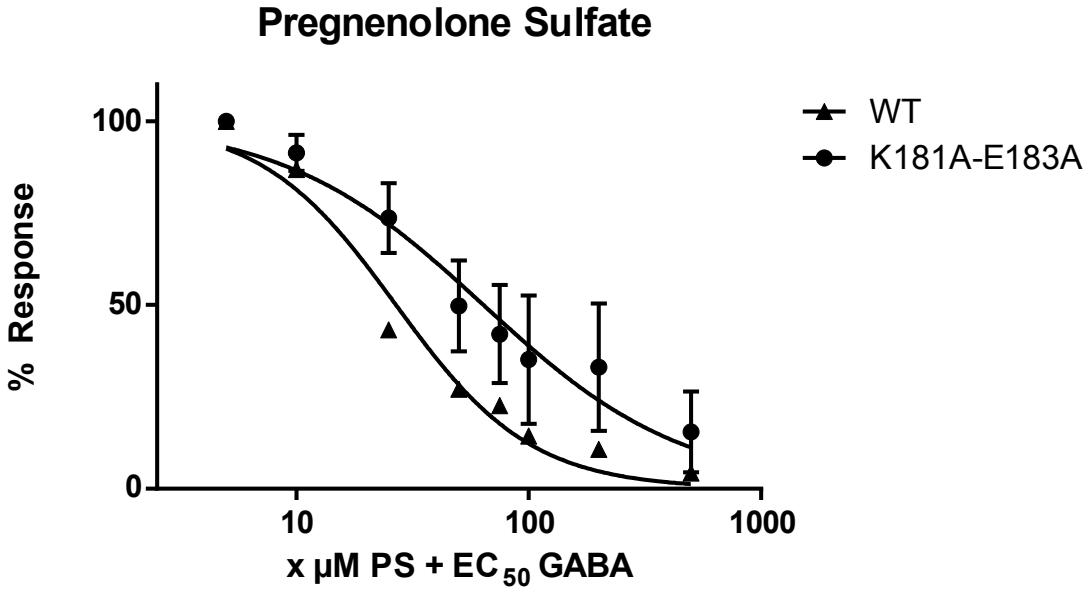

Figure 17: Dose response curve for the NAM pregnenolone sulfate tested on the K181A-E183A mutation of Hco-UNC-49B.

Table 3: A summary of EC_{50} and IC_{50} values for agonists and the NAM tested on the K181A and K181A-E183A mutations of Hco-UNC-49B

Mutant	Agonist	EC_{50} ± Standard Error (μM)	Hill Slope	Number of Oocytes
Wildtype UNC-49B/C	GABA	113 ± 10.83	1.54	15
	S-GABOB	382 ± 22*	1.11	6
	R-GABOB	234 ± 43*	1.67	6
	IMA	175 ± 21*	1.93	11
	DAVA	3914 ± 520*	1.47	7
K181A	GABA	252.9 ± 40.72	1.22	9
	S-GABOB	2111 ± 194.69	2.98	7
	R-GABOB	882.5 ± 186.01	1.49	6
	IMA	208.1 ± 18.74	1.20	4
K181A-E183A	GABA	114.7 ± 7.48	2.73	8
	IMA	207.2 ± 30.38	0.92	4
	DAVA	3429 ± 400.3	1.20	4

*Kaji et al. (2015)

Mutant	NAM	IC_{50} ± Standard Error (μM)	Hill Slope	Number of Oocytes
Wildtype UNC-49B/C	PS (IC_{50})	26.83 ± 0.39	-1.50	5
K181A-E183A		65.25 ± 24.58	-0.96	6

3.8 Disulfide Trapping

The disulfide trapping experiment was conducted to further understand the interaction between K181 and E183 as well as their potential effects on GABA binding in the Hco-UNC-49BC receptor. The goal was to determine the % inhibition of the receptor following the introduction of a disulfide bridge between two cysteine residues by washing with the oxidizing agent hydrogen peroxide (H_2O_2). Recordings were obtained from a minimum of 3 *X. laevis* oocytes from at least 2 different frogs. The results demonstrated a 23.22% ± 3.71 (n=5) inhibition in the double-cysteine mutant and a 5.9% ± 5.61 (n=5) inhibition in the K181C mutant following H_2O_2 exposure. The wildtype and E183C mutation did not display any inhibition in channel function, but rather showed an increase in channel response following H_2O_2 exposure. Wildtype showed a 6.27% ± 2.27

(n=3) increase in GABA response and E183C showed an 18.28% ± 9.94 (n=4) increase in GABA response. Treatment with DTT following the second GABA wash removed the introduced disulfide bond and GABA responses returned to similar levels seen before H_2O_2 exposure.

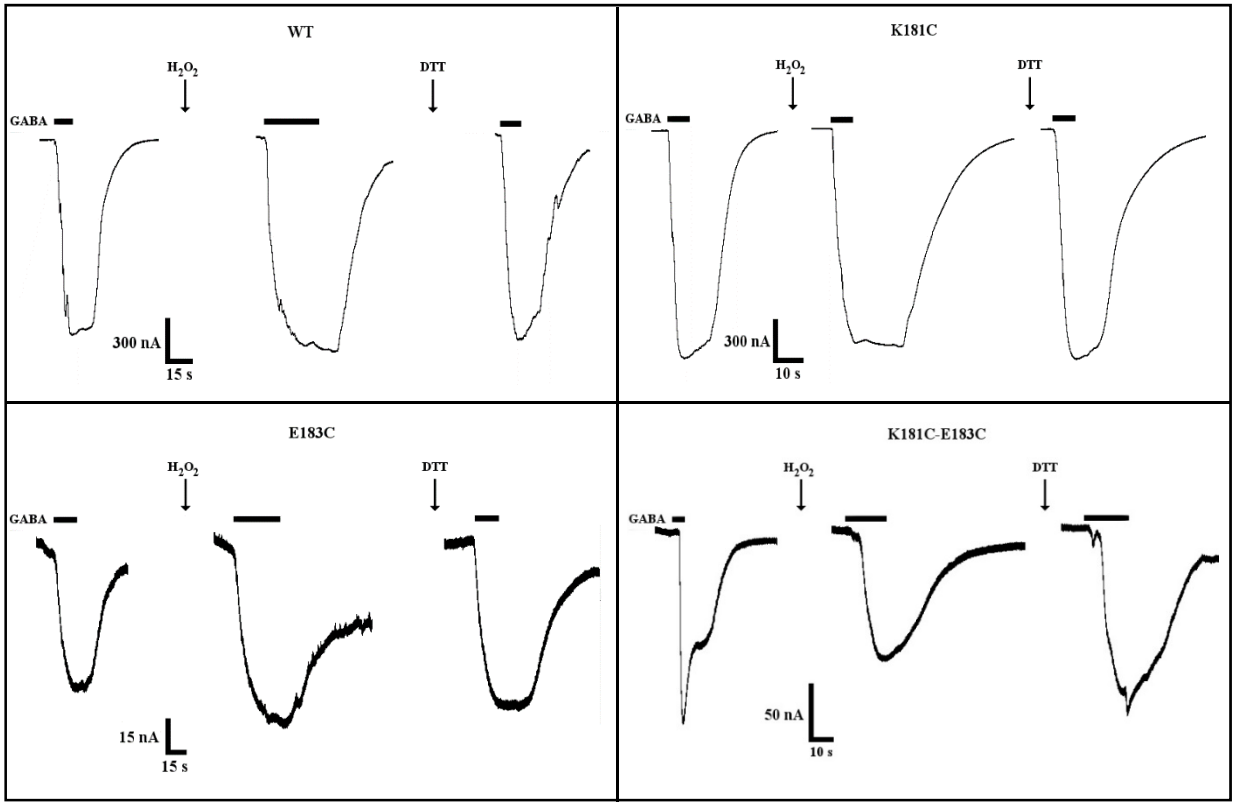

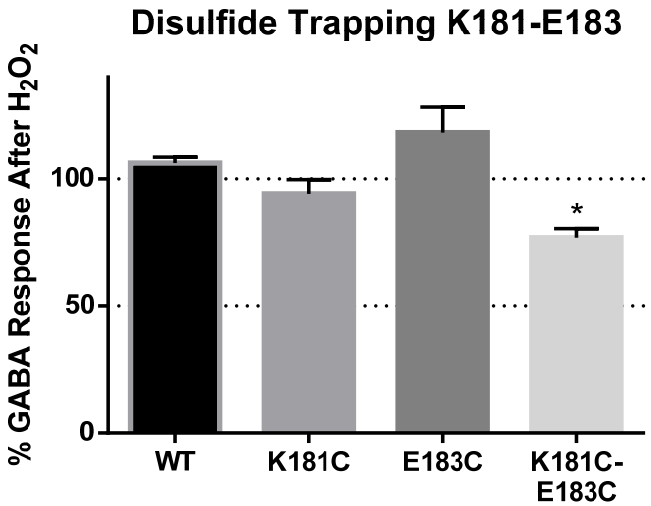

Figure 18: Disulfide trapping experiments conducted on various cysteine mutations in Hco-UNC-49B.

Representative electrophysiological traces and recorded responses to GABA following H_2O_2 exposure can be seen in Figure 18. The results from wildtype and both individual mutations were significantly different from the double mutation ($p<0.05$).

3.9 Mutant Cycle Analysis

With the electrophysiology results collected for the K181 and E183 mutations, further analysis was required to determine if these two residues interact with each other. Each mutation introduced to a protein structure is thought to result in a change in free energy (ΔG) of the overall structure which can influence protein folding. These changes can be visualized in Figure 19. Mutations in various positions are likely to affect the protein differently. A mutation involving two residues that do not interact is expected to have a change in free energy equal to the sum of both individual mutations, as each mutation has an additive impact on the overall structure.

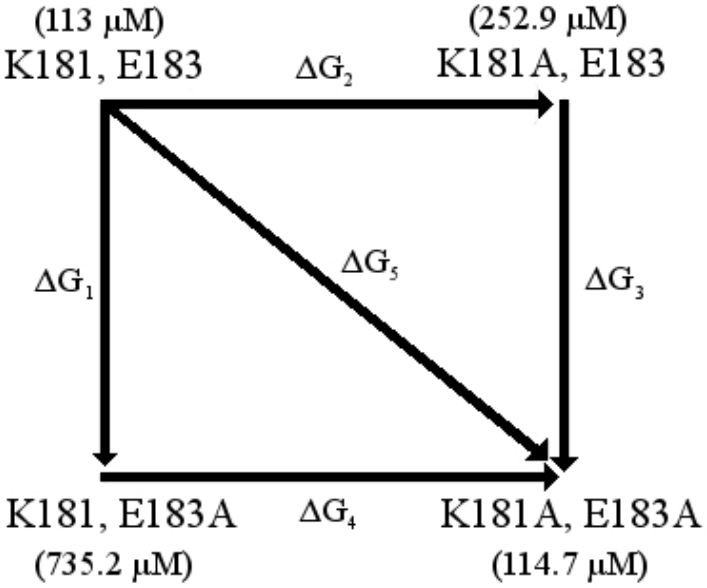

Figure 19: Visualization of the changes in free energy associated with K181/E183 mutations. EC_{50} values for each variant are presented in brackets.

However, two residues that interact may not show the same result. K181 and E183 mutations in Hco-UNC-49B had a negative effect on channel function and reduced the EC_{50} for GABA. Due to these two residues having opposite charge and a close proximity to each other, it is hypothesized that they interact and are important for channel functionality. Mutant cycle analysis revealed a non-additive change in free energy between the individual K181A and E183A mutations, and the combined K181A-E183A double mutation. Calculated changes in free energy and interaction energy can be seen in Table 4.

Table 4: Mutant cycle analysis of K181 and E183 residues in Hco-UNC-49B.

Mutant	**ΔG (kcal/mol)**	**ΔΔG (kcal/mol)**
K181A	0.48	n/a
E183A	1.11	n/a
K181A-E183A	0.01	(-) 1.58

Discussion

Section 4: Discussion

The goal of this thesis is to further characterize the GABA receptor, Hco-UNC-49, that is unique to the parasitic nematode *Haemonchus contortus*. The results may provide a better understanding of how the receptor functions and to help identify similarities and differences with other LGICs (vertebrate and invertebrate). Through the use of a model created using a *C. elegans* GluCl channel crystal structure as the template, a variety of individual amino acid residues within close proximity of the GABA binding site were selected. Selections were determined based on sequence homology with other GABA receptors such as the Human $GABA_A$ receptor, the *D. melanogaster* RDL receptor, and UNC-49 receptors found in other parasitic nematodes such as *B. malayi*, *T. pseudospiralis*, and *T. canis*. Single or double point mutations allowed specific modifications to be analyzed with TEVC electrophysiology to determine the impact and importance of each residue for the channel's overall function.

It is suspected that charged residues in loops B and C of the $GABA_A$ receptor are able to form salt bridges that are critical for GABA activation of the channel (Venkatachalan & Czajkowski, 2008). These interacting residues are thought to have a critical role in the transition of the channel from the closed to open state, specifically in positioning and stabilizing loop C upon ligand binding (Venkatachalan & Czajkowski, 2008).

Previous studies have identified the importance of several key residues in the $GABA_A$ receptor. Newell et al. (2004) demonstrated that the glutamic acid in position 155 of the β2 subunit in the $GABA_A$ receptor is crucial for modulation of channel opening following GABA binding. This residue is analogous to the E185 residue in the

Hco-UNC-49 receptor. Ashby et al. (2012) further demonstrated that a similar residue in the *D. melanogaster* RDL receptor, E204 (analogous to E185 in Hco-UNC-49), maintained an ionic interaction directly with the amino group of a bound GABA molecule. Past research in this lab by Josh Foster demonstrated that any mutations to the E185 residue in Hco-UNC-49 would render the channel non-functional as indicated by a lack of GABA response at less than 20 mM. Miller et al. (2014) further analyzed residues in the $GABA_A$ receptor that were thought to interact with the critical E155 residue and found that closure of the GABA binding site is maintained by salt bridge interactions between E153, R207, and E155. The *D. melanogaster* RDL receptor contains the same 3 interacting analogous residues at positions E202, E204, and R256, which are also important for function of that receptor (Ashby et al., 2012). The E153, E155, and R207 residues in the $GABA_A$ receptor and the E202, E204, and R256 residues in the RDL receptor are analogous to the E183, E185, and R241 residues found in the *H. contortus* UNC-49 receptor.

Venkatachalan & Czajkowski (2008) provided evidence for the existence of a salt bridge interaction between E153 and K196 in the human $GABA_A$ receptor. As previously mentioned, E153 in the $GABA_A$ β subunit is analogous to E183 in the *H. contortus* UNC-49B subunit. However, the UNC-49B subunit does not have a lysine, but rather a threonine, in the analogous position to K196. There is instead a lysine residue located at position 181 in the UNC-49B subunit, extremely close to the glutamic acid at 183. Model analysis revealed that these two residues are within close enough proximity (2.7Å) to form a salt bridge (Figure 20). An interaction like this within the GABA binding pocket could be important for receptor function, either by interacting with the ligand itself or

with nearby residues. The model also showed that a threonine in the T230 position is within close proximity of both K181 and E183 (4.2Å and 2.8Å respectively). Sequence alignment revealed that this T230 residue is highly conserved among other parasitic nematodes, however it is not found in the human $GABA_A$ receptor. Interestingly, in the human receptor these residues are swapped, with a threonine in the 181 position and a lysine in the 230 position. In an effort to create a salt-bridge analogous to the human E153 and K196, a double mutation (K181T, T230K) was introduced. This essentially removed the lysine residue from position 181 to allow E183 to potentially interact with the newly introduced lysine at position 230. Interestingly, this receptor was essentially non-functional. If this new salt bridge was in fact formed, it seems that in the nematode UNC-49 receptor it is not tolerated.

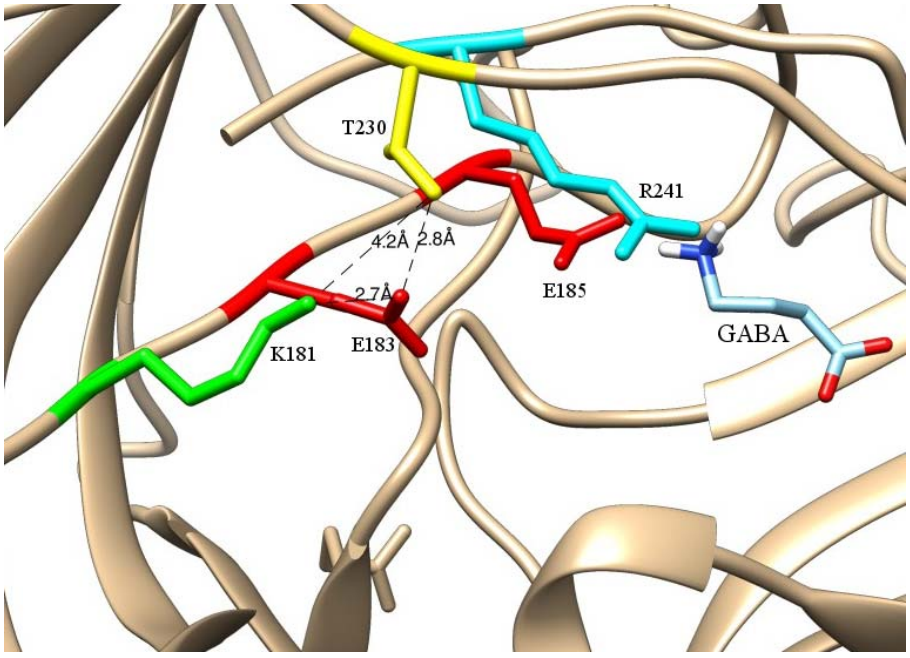

Figure 20: Key residues of the Hco-UNC-49 receptor with a GABA molecule docked in the binding site. Distances between potentially interacting residues are visualized with dotted lines.

The research presented in this thesis supports the idea of an important molecular interaction between the residues K181 and E183, and possibly with T230. Mutant cycle analysis between K181 and E183 reveals that these two residues are energetically linked in some way with an interaction energy ($\Delta\Delta G$) of (-) 1.58 kcal/mol. Compared to wildtype, the K181A mutation had a change in free energy (ΔG) of 0.48 kcal/mol, the E183A mutation had a ΔG of 1.11 kcal/mol, and the K181A-E183A mutation had a ΔG of 0.01 kcal/mol. Since the change in free energy associated with the double alanine mutation is not equal to the sum of the free energy changes occurring in the individual K181A and E183A mutations, it is highly likely that these two residues are interacting with each other (Venkatachalan & Czajkowski, 2008).

Though it is not clear exactly what role the K181 residue plays in channel activation, it is abundantly clear that the E183 residue is important for receptor functionality as every mutation in this position had a negative impact on the channel. Responses varied from a 6.5-fold decrease in GABA sensitivity with the E183A mutation up to an over 20-fold decrease in GABA sensitivity with the E183C mutation. Mutations to the K181 residue yielded less conclusive results, with almost all mutations at this position having a smaller negative impact on channel functionality. The least impactful change at this position was the K181C mutant, which had an EC_{50} that was not significantly different from the wildtype receptor ($p>0.05$). Additionally, the K181R mutation yielded an EC_{50} over 2-fold greater than that of the wildtype receptor, but the difference was not statistically significant ($p>0.05$). This is not entirely surprising since although arginine contains a larger guanidium group, it maintains a positive charge

similar to the amino group found in lysine, which could maintain an electrostatic interaction with E183. The most impactful change at this position was the K181E mutation, a single point charge reversal that resulted in a nearly 7-fold decrease in GABA sensitivity, suggesting that an electrostatic interaction with E183 may be assisting with channel activation and stability. The K181T mutation resulted in a statistically different ($p<0.05$) 2-fold reduction in GABA sensitivity from the wildtype receptor with an EC_{50} of 343.5 μM, but was able to show that an uncharged polar residue in the 181 position is still able to retain channel functionality at a reduced sensitivity.

The K181A-E183A mutation displayed a very interesting result in that its response to GABA was very similar to the wildtype receptor. It is unusual that each individual mutation (K181A and E183A) resulted in reduced GABA sensitivity with EC_{50} values of 252.2 μM and 735.2 μM respectively, yet both mutations occurring simultaneously produced an EC_{50} similar to wildtype (114.7 μM). One possibility is that these two residues are interacting to stabilize each other and potentially maintaining molecular interactions with other nearby residues. A removal of the positive charge on K181 could result in the E183 residue slightly shifting in orientation resulting in new or altered secondary interactions that affect the channel negatively. The presence of a salt bridge between K181 and E183 could prevent E183 from interfering with E185, which has been shown to be crucial for receptor function and is also thought to have a direct interaction with bound GABA molecules (Newell et al., 2004). This idea is supported by the double alanine mutation which has no apparent impact on GABA binding, since both positive and negative charges have been removed simultaneously. With both charges nullified, neither K181 nor E183 are able to interfere with nearby residues. The E183K mutation,

with an EC_{50} of 1155 μM, also suggests that potential interference with E185 could result in reduced channel functionality. Though the distance between E183 and E185 (5.02Å) is slightly further than the 4Å distance thought to be required for salt bridge formation, it is possible that the E183K mutation could position a lysine residue close enough to E185 to interfere with its existing interactions, such as with nearby residues or a bound GABA molecule.

Interestingly, the double alanine mutation displayed similar responses compared to wildtype when tested with the GABA agonists IMA and DAVA, but showed a different response when GABA inhibition was tested with PS. Further testing would be required to fully understand this interaction, but it is clear that there are some unique properties in the double alanine mutation that separate it from the wildtype receptor. Similarly with the single alanine mutation, K181A, the GABA agonist IMA displayed a response very close to that of the wildtype receptor. The other agonists tested on this mutant, R-GABOB and S-GABOB, displayed heavily decreased responses compared to wildtype. Both of these compounds contain a hydroxyl group on the third carbon. The model suggests that the hydroxyl group would be oriented towards the 181-185 residues during binding, and since that group is not found on either GABA or IMA, it could be the cause of the differences in agonist response.

The disulfide trapping experiment conducted on cysteine mutations in the K181 and E183 positions of Hco-UNC-49B was meant to determine if an interaction between these two residues is possible and to measure their effect on channel activation. Venkatachalan & Czajkowski (2008) conducted a similar experiment and found that residues in the $GABA_A$ receptor (E153 and K196) were responsible for regulating movement of loop C

following GABA binding. Only one of these residues is analogous to the *H. contortus* receptor (E183), but the K181 residue is within a close enough distance to have a similar salt bridge interaction. This experiment confirmed that these two residues have the potential to interact with each other based on their ability to form a disulfide bond when both mutated to cysteine residues. Hydrogen peroxide exposure which induces disulfide bond formation resulted in a 23.22% decrease in GABA sensitivity in the K181C-E183C double mutation. Based on these results, it is possible that K181 and E183 are also partly responsible for initiating the conformational change required to open the channel and allow ion passage following GABA binding.

The T230 residue appears to have some importance for the Hco-UNC-49 channel. Mutation to a lysine in this position resulted in a significant, over 11-fold decrease in GABA sensitivity, while a swap mutation with K181 rendered the channel non-functional with no responses at physiologically relevant levels. Since threonine is not an electrically charged amino acid, and the distance between K181 and T230 is above 4Å, there would not be a salt bridge interaction between these two residues. There may however be another form of molecular interaction occurring here that is vital for channel function. Further research would be required to better understand this relationship, but it does appear to be vital for the Hco-UNC-49 receptor.

Conclusion

Section 5: Conclusion

Previous and current work in the Forrester lab have provided a strong baseline for characterization of the Hco-UNC-49 receptor. It has been previously demonstrated that the invertebrate GABA receptor has key differences from the vertebrate receptor, such as excitatory GABA receptors responsible for intestinal waste expulsion in nematodes (Schuske et al., 2004). Further characterization identified unique properties of the Hco-UNC-49 receptor compared to other invertebrates such as *C. elegans*. Specifically, both species contain homomeric and heteromeric GABA receptors, yet they have displayed opposite trends in GABA sensitivity (Siddiqui et al., 2010). Several residues critical for receptor function have been identified within Hco-UNC-49 and mutations have been analyzed for their impact on GABA binding and overall channel efficiency.

The primary focus of this thesis is the potential interaction found between K181 and E183 in the B subunit of the Hco-UNC-49 receptor. These residues can be found in close proximity to the bound GABA molecule based on the model, are opposite in electrical charge, and are positioned within a short enough distance to form a salt bridge with each other. Mutations to K181 generally resulted in reduced GABA sensitivity, but did not have nearly as much of a negative impact on the channel as mutations in E183. The charge reversal mutation also reduced GABA sensitivity significantly, but none of the mutations in these two positions rendered the channel non-functional. Based on research conducted on analogous residues in other receptors such as human $GABA_A$, and the research conducted in this thesis, it appears that E183 is important for channel functionality. Other research in this thesis, such as the mutant cycling and disulfide trapping experiments described previously, strongly suggest the presence of a molecular

interaction between K181 and E183. It is possible that K181 may serve as a form of stabilization for E183, which explains why direct mutations on E183 have a larger negative impact on the channel.

Another goal of this thesis was to investigate the Hco-UNC-49 T230 residue after sequence homology revealed it is conserved among multiple invertebrate GABA receptors, yet not found in the human receptor. Conversely, the K181 residue is found in several invertebrates, but is replaced by a threonine in the human receptor. Similar to the K181-E183 interaction, mutations to the K181 residue slightly reduced GABA sensitivity, and mutating T230 had a much larger negative impact on the channel. Swapping K181 with the T230 residue rendered the channel non-functional. These results suggest that the T230 residue is very important for the Hco-UNC-49 receptor, though further analysis would be required to more precisely determine its role.

This thesis has revealed some new potential interactions and important individual residues within the unique Hco-UNC-49 GABA receptor that may prove to be useful in future pharmaceutical research. The residues highlighted here may assist with determining useful targets for new anthelmintics to help combat the growing *H. contortus* resistance concerns among countries that rely on ruminant animals for survival and economic growth. There are still more studies that can be conducted to better understand how this GABA receptor functions, but it has proven to be a good target and unique opportunity for anthelmintic research.

References

Section 6: References

Accardi, M. V. & Forrester, S. G. (2011). The *Haemonchus contortus* UNC-49B subunit possesses the residues required for GABA sensitivity in homomeric and heteromeric channels. *Molecular & Biochemical Parasitology*, 178, 15-22.

Accardi, M. V., Beech, R. N. & Forrester, S. G. (2012). Nematode cys-loop GABA receptors: biological function, pharmacology and sites of action for anthelmintics. *Invertebrate Neuroscience,* 12, 3-12.

Akkari, H., Jebali, J., Gharbi, M., Mhadhbi, M., Awadi, S., & Darghouth, M. A. (2013). Epidemiological study of sympatric *Haemonchus* species and genetic characterization of *Haemonchus contortus* in domestic ruminants in Tunisia. *Veterinary Parasitology*, 193(1-3), 118-125.

Ashby, J. A., McGonigle, I. V., Price, K. L., Cohen, N., Comitani, F., Dougherty, D. A., Molteni, C. & Lummis, S. C. R. (2012). GABA binding to an insect GABA receptor: A molecular dynamics and mutagenesis study. *Biophysical Journal*, 103, 2071-2081.

Bamber, B. A., Twyman, R. E. & Jorgensen, E. M. (2003). Pharmacological characterization of the homomeric and heteromeric UNC-49 GABA receptors in *C. elegans*. *British Journal of Pharmacology*, 138, 883-893.

Bamber, B., Beg, A. A., Twyman, R. E. & Jorgensen, E. M. (1999). The *Caenorhabditis elegans unc-49* locus encodes multiple subunits of a heteromeric GABA receptor. *The Journal of Neuroscience*, 19(13), 5348-5359.

Blackhall W. J., Prichard, R. K. & Beech, R. N. (2008). P-glycoprotein selection in strains of *Haemonchus contortus* resistant to benzimidazoles. *Veterinary Parasitology*, 152, 101-107.

Blaxter, M. L., De Ley, P., Garey, J. R., Liu, L. X., Scheldeman, P., Vierstraete, A., Vanfleteren, J. R., Mackey, L. Y., Dorris, M., Frisse, L. M., Vida, J. T. & Thomas, K. (1998). A molecular evolutionary framework for the phylum Nematoda. *Nature*, 392(5), 71-75.

Boulin, T., Fauvin, A., Charvet, C. L., Cortet, J., Cabaret, J., Bessereau, J-L & Neveu, C. (2011). Functional reconstitution of *Haemonchus contortus* acetylcholine receptors in *Xenopus* oocytes provides mechanistic insights into levamisole resistance. *British Journal of Pharmacology*, 164, 1421-1432.

Carter, P. J., Winter, G., Wilkinson, A. J. & Fersht, A. R. (1984). The use of double mutants to detect structural changes in the active site of tyrosyl-tRNA synthetase (*Bacillus stearothermophilus*). *Cell*, 38(3), 835-840.

Cascio, M. (2004). Structure and function of the glycine receptor and related nicotinicoid receptors. *The Journal of Biological Chemistry*, 279(19), 19383-19386.

Charvet, C. L., Robertson, A. P., Cabaret, J., Martin, R. J. & Neveu, C. (2012). Selective effect of the anthelmintic bephenium on *Haemonchus contortus* levamisole-sensitive acetylcholine receptors. *Invertebrate Neuroscience*, 12, 43-51.

Dougherty, D. A. (2007). Cation-pi interactions involving aromatic amino acids. *Journal of Nutrition*, 137, 1504S-1508S.

Elgart, G. W. & Meinking, T. L. (2003). Ivermectin. *Dermatologic Clinics*, 21, 277-282.

Gurdon, J. B., Lane, C. D. & Woodland, H. R. (1971). Use of frog eggs and oocytes for the study of messenger RNA and its translation in living cells. *Nature*, 233(5316), 177-182.

Horovitz, A. (1996). Double-mutant cycles: a powerful tool for analyzing protein structure and function. *Folding and Design*, 1(6), R121-R126.

Jones, K. A., Borowsky, B., Tamm, J. A., Craig, D. A., Durkin, M. M., Dai, M., Yao, W., Johnson, M., Gunwaldsen, C., Huand, L., Tang, C., Shen, Q., Salon, J. A., Morse, K., Laz, T., Smith, K. E., Nagarathnam, D., Noble, S. A., Branchek, T. A. & Gerald, C. (1998). $GABA_B$ receptors function as a heteromeric assembly of the subunits $GABA_BR1$ and $GABA_BR2$. *Nature*, 396(17), 674-679.

Kaji, M. D., Kwaka, A., Callanan, M. K., Nusrat, H., Desaulniers, J. & Forrester, S. G. (2015). A molecular characterization of the agonist binding site of a nematode cys-loop GABA receptor. *British Journal of Pharmacology*, 172, 3737-3747.

Komuniecki, R., Law, W. J., Jex, A., Geldhof, P., Gray, J., Bamber, B. & Gasser, R. B. (2012). Monoaminergic signaling as a target for anthelmintic drug discovery: Receptor conservation among the free-living and parasitic nematodes. *Molecular & Biochemical Parasitology*, 183, 1-7.

Manninen, S. & Oksanen, A. (2010). Haemonchosis in a sheep flock in North Finland. *Acta Veterinaria Scandinavica*, 52, S19.

Martin, R. J., Robertson, A. P. & Bjorn, H. (1997). Target sites of anthelmintics. *Parasitology*, 114, S111-S124.

Miller, P. S. & Aricescu, A. R. (2014). Crystal structure of a human $GABA_A$ receptor. *Nature*, 512(7514), 270-275.

Newell, J. G., McDevitt, R. A. & Czajkowski, C. (2004). Mutation of glutamate 155 of the $GABA_A$ receptor β_2 subunit produces a spontaneously open channel: A trigger for channel activation. *The Journal of Neuroscience*, 24(50), 11226-11235.

Newton, S. E. (1995). Progress on vaccination against *Haemonchus contortus*. *International Journal for Parasitology*, 25(11), 1281-1289.

Nikolaou, S. & Gasser, R. B. (2006). Prospects for exploring molecular developmental processes in *Haemonchus contortus*. *International Journal for Parasitology*, 36, 859-868.

Olsen, R. W. & DeLorey, T. M. (1999). GABA Synthesis, Uptake and Release. Basic Neurochemistry: Molecular, Cellular and Medical Aspects. 6th edition.

Qamar, M. F., Maqbool, A., & Ahmad, N. (2011). Economic losses due to haemonchosis in sheep and goats. *Science International,* 23(4), 321-324.

Schuske, K., Beg, A. A. & Jorgensen, E. M. (2004). The GABA nervous system in *C. elegans*. *TRENDS in Neurosciences*, 27(7), 407-414.

Sherman-Gold, R. (1993). The AXON guide for electrophysiology and biophysics laboratory techniques, Chapter 3. AXON Instruments Inc. pp26-81.

Siddiqui, S. Z., Brown, D. D. R., Rao, V. T. S. & Forrester, S. G. (2010). An UNC-49 GABA receptor subunit from the parasitic nematode *Haemonchus contortus* is associated with enhanced GABA sensitivity in nematode heteromeric channels. *Journal of Neurochemistry,* 113, 1113-1122.

Sieghart, W. (1995). Structure and pharmacology of gamma-aminobutyric $acid_A$ receptor subtypes. *Pharmacological Reviews*, 47(2), 181-234.

Sobczak, K., Bangel-Ruland, N., Leier, G. & Weber, W. (2010). Endogenous transport systems in the *Xenopus laevis* oocytes plasma membrane. *Methods*, 51, 183-189.

Thompson, A. J., Lester, H. A. & Lummis, S. C. R. (2010). The structural basis of function in cys-loop receptors. *Quarterly Reviews of Biophysics*, 43(4), 449-499.

Unwin, N. (1993). Neurotransmitter action: Opening of ligand-gated ion channels. *Cell*, 72, 31-41.

Unwin, N. (2005). Refined structure of the nicotinic acetylcholine receptor at 4A resolution. *Journal of Molecular Biology*, 346, 967-989.

Unwin, N., Miyazawa, A., Li, J. & Fujiyoshi, Y. (2002). Activation of the nicotinic acetylcholine receptor involves a switch in conformation of the α subunits. *Journal of Molecular Biology*, 319, 1165-1176.

Veglia, F. (1915). The anatomy and life-history of the *Haemonchus contortas*. *Veterinary Research Laboratories*.

Venkatachalan, S. P. & Czajkowski, C. (2008). A conserved salt bridge critical for $GABA_A$ receptor function and loop C dynamics. *Proceedings of the National Academy of Sciences of the United States of America*, 105(36), 13604-13609.

Zhang, D., Pan, Z., Awobuluyi, M. & Lipton, S. A. (2001). Structure and function of $GABA_C$ receptors: a comparison of native versus recombinant receptors. *TRENDS in Pharmacological Sciences*, 22(3), 121-132.

Appendices

Section 7: Appendices

Appendix A: D83 Mutations

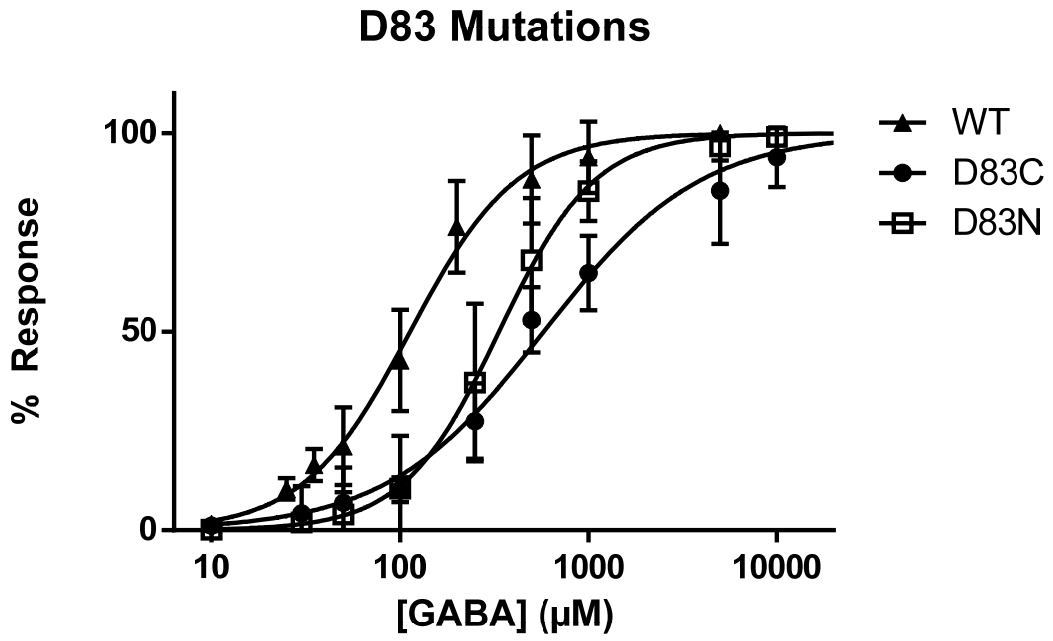

Figure 21: Dose response curves for mutations of Hco-UNC-49B in the D83 position.

Mutations in the D83 position were conducted to assist with Josh Foster's research in the investigation of a salt bridge between D83 and R159. Mutation of D83 to a cysteine resulted in an EC_{50} of 578.5 ± 116.59 (n=10), a 5-fold decrease in GABA sensitivity compared to wildtype. The mutation to asparagine (D83N) resulted in a 3-fold decrease in GABA sensitivity with an EC50 of 335.1 ± 48.90 (n=9). These results are displayed alongside the wildtype responses in Figure 21.

Appendix B: E131 Mutations

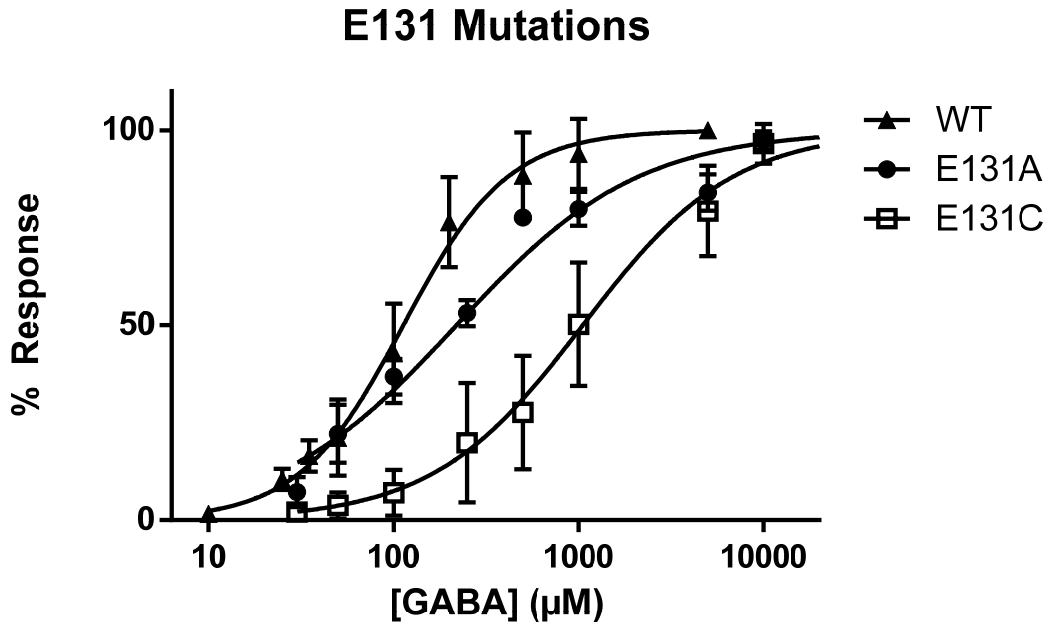

Figure 22: Dose response curves for mutations of Hco-UNC-49B in the E131 position.

Mutations in the E131 position were conducted to assist with Josh Foster's research in the investigation of another potential salt bridge between E131 and R159. Mutation to an uncharged alanine (E131A) resulted in a 2-fold decrease in GABA sensitivity with an EC50 of 219.1 ± 20.61 (n=5). The cysteine mutation (E131C) resulted in a large, 9-fold decrease in GABA sensitivity with an EC50 of 1054 ± 210.41 (n=11). Dose responses for these mutations can be seen in Figure 22.